Development of oxaalkyne and alkyne fatty acids as novel tracers to study fatty acid beta-oxidation pathways and intermediates

Lars Kuerschner*[ID] , Philipp Leyendecker[ID] , Kristina Klizaite, Maria Fiedler[ID] , Jennifer Saam[ID] , and Christoph Thiele[ID]

LIMES Life and Medical Sciences Institute, University of Bonn, Bonn, Germany

Abstract Fatty acid beta-oxidation is a key process in mammalian lipid catabolism. Disturbance of this process results in severe clinical symptoms, including dysfunction of the liver, a major beta-oxidizing tissue. For a thorough understanding of this process, a comprehensive analysis of involved fatty acid and acyl-carnitine intermediates is desired, but capable methods are lacking. Here, we introduce oxaalkyne and alkyne fatty acids as novel tracers to study the beta-oxidation of long- and medium-chain fatty acids in liver lysates and primary hepatocytes. Combining these new tracer tools with highly sensitive chromatography and mass spectrometry analyses, this study confirms differences in metabolic handling of fatty acids of different chain length. Unlike longer chains, we found that medium-chain fatty acids that were activated inside or outside of mitochondria by different acyl-CoA synthetases could enter mitochondria in the form of free fatty acids or as carnitine esters. Upon mitochondrial beta-oxidation, shortened acyl-carnitine metabolites were then produced and released from mitochondria. In addition, we show that hepatocytes ultimately also secreted these shortened acyl chains into their surroundings. Furthermore, when mitochondrial beta-oxidation was hindered, we show that peroxisomal beta-oxidation likely acts as a salvage pathway, thereby maintaining the levels of shortened fatty acid secretion. [JLR] Taken together, we conclude that this new method based on oxaalkyne and alkyne fatty acids allows for metabolic tracing of the beta-oxidation pathway in tissue lysate and in living cells with unique coverage of metabolic intermediates and at unprecedented detail.

Mitochondrial β-oxidation is the major degradation pathway for FAs in mammals and a key to understanding cellular energy balance ([1], [2]). This pathway is a complex process involving FA activation to an acyl-CoA, conversion to the corresponding acyl-CAR, transport into mitochondria, and regeneration of the acyl-CoA inside the mitochondria. These preparatory steps are finally followed by the actual β-oxidation sequence of enzymatic reactions. In the case of the long-chain FA palmitate, this comprises seven cycles of four enzymatic steps to release eight acetyl-CoA from the initial FA.

Medium-chain FAs containing 8–12 carbon atoms are subject to a rapid oxidative metabolism ([3], [4]). Unlike long-chain FAs, they may cross membranes in the nonesterified form ([5]–[7]). Medium-chain FAs are primarily catabolized in mitochondria, but like long-chain FAs may also undergo peroxisomal β-oxidation. Indeed, peroxisomes accommodate a related pathway that in mammals appears to be of greatest importance for the catabolism of very long-chain FAs and is independent of a carnitine-mediated transport ([6]–[9]). At both cellular organelles analogous intermediates are produced but by different enzymes. Although the single steps in β-oxidation are known, their coordinated interplay is not well understood, which is a consequence of the lack of an accessible method for comprehensive tracing of β-oxidation.

The classical assay on β-oxidation uses radioactive 1-^{14}C-palmitate ([10]). In this protocol, the radiolabeled FA is incubated with liver homogenate in the presence of ATP, CoA, and carnitine. After 5–60 min, the reaction is stopped by strong acidification, which precipitates unreacted palmitate together with protein. Radioactivity that is released as CO_2 (typically 20%) or in the aqueous supernatant (typically 80%) is quantified and indicates β-oxidation. The molecular identity of the radioactivity in the acid supernatant is usually not investigated and is assumed to be a mixture of acetyl-CoA and citric acid cycle intermediates. Also, the radioactive assay does not provide information about progress of oxidation beyond the first cycle. To improve the understanding of β-oxidation in cellular

systems, it appears necessary to trace in parallel the large number of different metabolites that are of rather different chemical properties.

Alkyne FAs represent a powerful alternate to radiolabeled FA tracers (11). These lipid probes contain a single terminal triple bond embedded in their hydrocarbon structure. With the advent of bioorthogonal chemistry (12) including click chemistry (13) the sensitive and specific detection of compounds containing terminal alkynes has become possible (14, 15). Clickable lipid tracers were successfully used to monitor protein lipidation, protein-lipid interaction, lipid localization, and metabolism, and this work has been extensively reviewed (16–20). Importantly, alkyne lipids are amenable to various highly sensitive detection procedures including TLC and MS-based lipidomics (11, 21–27). The versatility of the alkyne tag in combination with advanced click reporters, detection technologies, and instrumentation has opened new possibilities in lipid research. However, the particular developments in alkyne FA tracing have thus far focused on anabolic pathways (11, 22–25). For analysis of catabolism, the potential of alkyne FAs and the new methodologies has not been explored. In principal, the alkyne tracing technology also promises to deliver new details on β-oxidation.

The current study establishes alkyne FAs as a novel technique to study β-oxidation in mammalian tissue lysates and cells. It introduces a novel class of tracers, the oxaalkyne FAs, as a dedicated tool for this purpose. The applicability of the new approach is demonstrated by investigating liver catabolism of long-chain and medium-chain FAs.

MATERIALS AND METHODS

Synthesis of 11-Oxa-heptadec-16-ynoic acid (FA 17:0;Y;oxa)

1-Bromo-11-oxa-heptadec-16-yn: 5-Hexyn-1-ol (1.5 g, 15 mmol) was dissolved in 5 ml tetrahydrofuran. A solution of lithiumhexamethylenedisilazane (15 ml 1 M) in THF was slowly added at room temperature. After 5 min, a solution of 1,10-dibromodecane (6 g, 20 mmol) in 2 ml tetrahydrofuran and 8 ml dimethylformamide was added in one portion and the mixture allowed to react for 24 h at room temperature. Hexane (20 ml), diethylether (20 ml), and 5% citric acid in water (20 ml) were added. After shaking and phase separation, the upper phase was collected and the lower phase re-extracted with 20 ml hexane/ethyl acetate 1/1. The combined organic phases were dried and evaporated and the residue separated on a silica column with a gradient of 0%–10% ethyl acetate in hexane to yield 1.8 g (5.7 mmol, 38%) of the title compound. 1H-NMR (400 mHz, 20 mg/ml in CDCl₃): 3.37–3.48 (m, 6H, 1-,10-,12-CH₂), 2.24 (dt, 2H, 15-CH₂), 1.96 (t, 1H, 17-alkyne CH), 1.82–1.92 (m, 2H, 2-CH₂), 1.55–1.75 (m, 6H, 9-,13-,14-CH₂), 1.45 (m, 2H, 3-CH₂), 1.25–1.4 (m, 10 H, 4-8-CH₂).

11-Oxa-heptadec-16-ynoic acid (28). To a solution of 207 mg (3 mmol) sodium nitrite in 2 ml DMSO were added 0.6 ml (10 mmol) acetic acid and 320 mg (1 mmol) 1-bromo-11-oxa-heptadec-16-yn. The mixture was stirred in a closed tube for 24 h at 35°C. Hexane (5 ml), diethyl ether (3 ml), and 10% HCl (2 ml) were added. After shaking, the upper phase was collected, the lower phase re-extracted twice with hexane/ethyl acetate 1/1 and the combined organic phases washed with 5 ml water. To separate the carboxylic acid from the alkyl bromide and the corresponding alcohol, the organic phase was extracted twice with 15 ml water/methanol 3/1 while the pH of the mixture was adjusted to 8 using saturated NaHCO₃ solution. The extract was acidified with conc. HCl and extracted with 2x20 ml hexane/ethyl acetate 1/1. The extract was dried, evaporated and the residue purified on silica gel (hexane/ethyl acetate 3/1) to give 50 mg (19%) pure 11-oxa-heptadec-16-ynoic acid. Although the yield is moderate, the procedure is quick, simple and reliable. 1H-NMR (400 mHz, 20 mg/ml in CDCl₃): 3.37–3.48 (m, 6H, 1-,10-,12-CH₂), 2.37 (t, 2H, 2-CH₂), 2.23 (dt, 2H, 15-CH₂), 1.98 (t, 1H, 17-alkyne CH), 1.55–1.75 (m, 8H, 3-,9-,13-,14-CH₂), 1.45 (m, 2H, 3-CH₂), 1.25–1.4 (m, 10 H, 4-8-CH₂).

Synthesis of other oxaalkyne fatty acids

The synthesis of 9-oxa-pentadec-14-ynoic acid, 7-oxa-tridec-12-ynoic acid, and 5-oxa-undec-10-ynoic acid was performed analogous to the above synthesis. The assigned NMR spectra of the products and the intermediate bromides can be found in the supplementary information.

3-Oxa-non-8-ynoic acid was synthesized by treatment of 5-hexyn-1-ol with lithiumhexamethylenedisilazane as above and reaction of the lithiated alcohol with 2-bromoacetic acid in tetrahydrofurane/dimethylformamide. After washing and phase separation as above, the product was directly obtained by purification on silica using hexane/ethyl acetate 1/1. 1H-NMR (400 mHz, 20 mg/ml in CDCl₃): 4.17 (s, 2H, 2-CH₂), 3.62 (t, 2H, 4-CH₂), 2.26 (dt, 2H, 7-CH₂), 1.98 (t, 1H, 9-alkyne CH), 1.6–1.85 (2 × m, 4H, 5-,6-CH₂).

Synthesis of acyl carnitines

All acyl carnitines used in this study were prepared by acylation of anhydrous carnitine solutions (obtained by treatment of carnitine chloride in acetonitrile with stoichiometric amount of silver tetrafluoroborate) with the acyl chloride, followed by purification by silica gel chromatography and elution with pure chloroform and pure methanol as described (29). Identity was checked by HR-MS and MS/MS in the positive mode.

Preparation of liver lysate

Eight-week-old male C57BL/6N mice fed *ad libitum* were euthanized by cervical dislocation. The left lateral lobe of the liver was dissected and briefly rinsed in ice-cold STE buffer (10 mM Tris/HCl pH 7.4, 250 mM sucrose, 1 mM EDTA). In total, 440 mg tissue was homogenized in 20 ml STE buffer using a dounce tissue grinder with a loose-fitting pestle (Wheaton Science) by five down- and five up-strokes. The crude homogenate was centrifuged at 4°C and 450 *g* for 10 min. The supernatant was retrieved and used as lysate immediately.

β-Oxidation assay on whole liver lysate

The assay followed the literature (10) with minor adaptations. For a single reaction, 10 μl liver lysate was preincubated

with 80 µl assay buffer (10 mM Tris/HCl pH 8.0, 94 mM sucrose, 0.125 mM EDTA, 6.25 mM KH_2PO_4, 100 mM KCl, 1.25 mM $MgCl_2$, 2.5 mM L-carnitine, 0.125 mM L-malate, 65 µM CoA, 2.5 mM ATP, 1.25 mM DTT) in the absence or presence of 50 µM teglicar (Avanti) at 33°C for 10 min. The reaction was started by addition of prewarmed 10 µl FA solution (2 mM tracer in 7.7% delipidated BSA, Sigma) and incubation at 33°C C for 0–90 min. The reaction was stopped by addition of ice-cold 400 µl methanol/chloroform 2/1. This mix was subjected to both TLC and MS analysis. For the latter, an aliquot was directly dissolved in spray buffer (isopropanol/MeOH/H_2O 8/5/1 containing 10 mM ammonium acetate, 0.1% acetic acid, and the internal standards FA 16:0[(2,2)D2] and CAR 15:0) without prior click reaction. All assays comparing the various tracers in time series used the same lysate preparation and common stock solutions and were performed in parallel on the same day by the same experimenter.

β-Oxidation assay on liver lysate with subcellular fractionation

To enrich for mitochondria, the liver lysate was centrifuged at 4°C and 10,000 g for 10 min. The supernatant was collected as nonmitochondrial fraction. The pellet was resuspended trice using the dounce tissue grinder with a loose-fitting pestle and 1.5 ml ice-cold STE buffer followed by centrifugation at 4°C and 10,000 g for 10 min to yield the final suspension enriched in mitochondria. For a single reaction, 10 µl of the nonmitochondrial fraction or the suspension enriched in mitochondria was preincubated with 80 µl assay buffer in the absence or presence of 20 µM triacsin C (Sigma) at 37°C for 10 min. The reaction was started by addition of prewarmed 10 µl FA solution (1 mM tracer in 7.7% delipidated BSA, Sigma) and incubation at 37°C for 0–20 min. At the end of the incubation time, the suspension enriched in mitochondria was separated further. For that, the sample was incubated on ice for 3 min to halt the reaction, followed by centrifugation at 4°C and 10,000 g for 10 min. The supernatant was retrieved as extra-mitochondrial volume and the pellet as mitochondria fraction. The latter was mixed with 100 µl ice-cold methanol. To all other samples 400 µl ice-cold methanol were added to stop the reaction. If applying, the methanol contained CAR 13:0;Y as internal standard. This mix was subjected to click reaction and TLC analysis. All assays used the same lysate preparation and common stock solutions and were performed in parallel on the same day by the same experimenter.

Western blotting

The nonmitochondrial fraction and the suspension enriched in mitochondria were analyzed by SDS-PAGE and Western blotting using an antibody that detects ACSM1 (SAB2700719, Sigma).

Isolation of primary hepatocytes

The isolation of primary hepatocytes by collagenase perfusion followed the literature (25, 30) with minor adaptations (permission LANUV NRW, 84–02.04.2015.A381). Eight-week-old male C57BL/6N mice were injected with heparin-sodium (430 U in 100 µl, Ratiopharm) and anaesthetized with a ketamin/xylazin mixture. After cannulation (26G 0.6 × 19 mm cannula, BD Biosciences) of the portal vein, the liver was perfused at 4 ml/min sequentially with preperfusion buffer (Hanks' balanced salt solution, 5 mM EGTA pH 7.4, 25 U/ml heparin-sodium) for 2 min, followed by collagenase buffer (Williams medium E, 0.125 mM $CaCl_2$, 0.5 mg/ml collagenase NB46, Sigma) for 5 min. The liver was maintained at 37°C using a 150 W heat lamp and a thermometer (ATC2000, World Precision Instruments). Cells were released into 50 ml hepatocyte medium (Williams medium E, 10% FCS, 2 mM L-glutamine, 100 U/ml penicillin, 100 mg/ml streptomycin), and the cell suspension was centrifuged at 20 g for 2 min. The pellet, containing the primary hepatocytes, was resuspended in fresh hepatocyte medium, filtered through a 100 µm nylon cell strainer, and plated onto collagen-coated 12-well dishes at a density of 150,000 cells per well.

Lipid labeling of cells

Primary hepatocytes grown for 2 h were preincubated with 50 µM teglicar or DMSO in 800 µl of hepatocyte medium for 10 min. Labeling was performed in fresh 800 µl of hepatocyte medium containing 50 µM FA tracer and 50 µM teglicar or DMSO and cell incubation at 37°C for 5 min to 6 h. Growth medium was collected and frozen at 80°C. Cells were washed once with ice-cold hepatocyte medium and once with ice-cold PBS. Upon complete removal of all liquid, the plates were frozen at 80°C until lipid extraction.

Lipid extraction from hepatocytes and growth media

The procedure followed the literature (25) with minor adaptations. Cellular lipids were extracted by sonication of multiwell plates in MeOH/$CHCl_3$ 5/1 containing internal standards (Cer 18:0;O2/15:1(11Z)[(12,13,14,15)D8]; DG 17:0;Y_15:1(11Z)[(12,13,14,15)D8]; PA 17:0;Y/15:1(11Z)[(12,13,14,15)D8]; PC 17:0;Y/15:1(11Z)[(12,13,14,15)D8]; PE 17:0;Y/15:1(11Z)[(12,13,14,15)D8]; PI 17:0;Y/15:1(11Z)[(12,13,14,15)D8]; PS 17:0;Y/15:1(11Z)[(12,13,14,15)D8]; SE[(26,27D6)] 17:0;Y; TG 16:0_17:0;Y_15:1(11Z)[(12,13,14,15)D8] all ref. (24); TG 17:0;Y_17:0;Y_15:1(11Z)[(12,13,14,15)D8]; CAR 15:0; DG 14:0_17:1; MG 17:1; PA 14:0/17:1; PC 14:0/17:1; PE 14:0/17:1; PI 17:0/17:0; PS 14:0/17:1; SE 17:1; TG 18:1_16:0[D2]_16:0[D2]; FA 16:0;Y[(1,2,3,4,5,6,7,8,9)13C9] and commercially available Cer 17:0; GlcCer 12:0; LPA 17:0; LPC 17:1; LPE 17:0; PG 28:0; SM 17:0; FC 27:1;O[(26,27)D6] (all Avanti); FA 16:0[(2,2)D2] (Cambridge Isotope); NeuAcHex2Cer 42:1;O2[D3] (Cayman chemical) as well as either CAR 13:0;Y or CAR 13:0;Y;oxa) for subsequent MS quantification. An aliquot of the growth media was extracted alike but using MeOH/$CHCl_3$ 3/1 containing the internal standards. Proteins precipitating from the one-phase mix were removed before a two-phase separation of lipids. The dried lipids were redissolved in $CHCl_3$ and subjected to both TLC and MS analysis.

Click-reaction of alkynes and TLC analysis

The protocol followed the literature (11) with minor adaptations. For liver lysates, the stopped assay mix was centrifuged 20,000 g for 2 min and 5 or 10 µl of the supernatant were incubated with 40 µl of coumarin mix (10 µl 3-azido-7-hydroxycoumarin (2 mg/ml in acetonitrile), 250 µl of 10 mM Cu(I)BF_4 in acetonitrile, 850 µl of EtOH) overnight at 43°C in a heating block. For hepatocytes, an aliquot of the lipids of cells or growth media was incubated with 40 µl of coumarin mix. Synthetic alkyne-labeled lipids serving as standards for TLC were coprocessed. After the click reaction, samples were separated by TLC on HPTLC plates (Merck) using two solvent mixes sequentially (solvent I: $CHCl_3$/MeOH/H_2O/acetic acid 60/40/5/1; solvent II: hexane/ethyl

acetate 1/1), dried and briefly soaked in 4% N,N-diisopropylethylamine in hexane). Fluorescence images of TLC plate illuminated by a 420 nm light source were acquired with a Rolera MGI plus EMCCD camera (Decon Science Tec), equipped with a 494/20 nm emission filter, all under control of GelPro analyzer (Media Cybernetics) software. Densitometry analysis was performed using GelAnalyzer software v19.1 (www.gelanalyzer.com).

Click-reaction of alkynes from hepatocytes and growth media for MS analysis

Analyses were performed using the standard protocol described before (24). Briefly, 10 μl of above lipid extracts were incubated with 40 μl of reaction mixture (10 μl of 100 mM of C171 in 50% MeOH, 100 μl of 10 mM Cu(I)-TFB in acetonitrile, 900 μl 100% EtOH) at 40°C for 16 h. After the click reaction, the samples were subjected to two-phase separation using chloroform and water. The lipids of the dried chloroform phase were dissolved in spray buffer (isopropanol/MeOH/H₂O 8/5/1 containing 10 mM ammonium acetate, 0.1% acetic acid).

MS analysis

Mass spectra were recorded on a Thermo Q-Exactive Plus spectrometer equipped with a robotic TriVersa NanoMate (Advion Biosciences). Aliquots of lipid extracts in spray buffer (isopropanol/MeOH/H₂O 8/5/1 containing 10 mM ammonium acetate, 0.1% acetic acid) were infused using a back-pressure of 0.9 psi and ionization voltage of ±1.1 kV and analyzed in positive or negative ion mode. MS1 spectra (resolution 280,000) were recorded in 100 m/z windows from 200 to 1400 m/z (positive mode) or 100–400 m/z (negative mode) followed by recording MS/MS spectra (resolution 140,000 or 70,000) by data independent acquisition in 0.5 or 1 m/z windows from 200 to 1,200 m/z (positive mode) or 100–400 m/z (negative mode).

MS data analysis

Raw files were converted to mzml files using MSConvert and analyzed using LipidXplorer (31). For identification and quantification of alkyne and oxaalkyne lipids, molecular fragment query language (mfql) files were written, which identify each lipid species by the presence of its expected mass peak and, if applicable, the occurrence of the characteristic fragment peak. Lipids were quantified using the respective internal standard (see supplementary information for details).

RESULTS

Tracer conceptualization

Upon complete β-oxidative processing, an alkyne FA yields a short chain terminally unsaturated CoA thioester. Accordingly, the alkyne analogue of palmitate, FA 17:0;Y, results in metabolic generation of propiolyl-CoA (Fig. 1A). This end product has been found instable (32) and thus escapes faithful detection and quantification.

To benefit from the power of alkyne lipid tracing also in experiments analyzing FA catabolism, we conceived a novel set of alkyne FA probes, oxaalkyne FAs, which carry an oxygen atom within the hydrocarbon chain (Fig. 1B). We reasoned that during β-oxidation the substituting oxygen would eventually locate to the γ-position of the shortened chain to arrest further processing. During tracer design we opted for a placement of the oxygen to the ω-7 position, which correspondingly would result in the accumulation of the FA 9:0;Y;oxa catabolite. This design promised a stable alkyne moiety within a metabolic end product that can be reliably identified and quantified. The number of possible oxidation cycles would depend on the original chain length of the oxaalkyne FA tracer. The activity of FA catabolism could be measured by analyzing the level of FA 9:0;Y;oxa in a sample.

Long-chain FA β-oxidation in liver lysate

To evaluate the applicability of alkyne and oxaalkyne FAs for investigations on FA catabolism, we first assayed β-oxidation in murine liver homogenates using TLC separation and fluorescence imaging (Fig. 1C–F). An alkyne (Fig. 1C) or oxaalkyne (Fig. 1D) analogue of the saturated palmitic acid was incubated with fresh liver lysate for different times in a widely used experimental setup (10).

The input alkyne tracer FA 17:0;Y yielded the only detectable band at time point 0 min (Fig. 1C). Its signal remained prominent for the first 15 min of incubation time before fading strongly. The main metabolite CAR 17:0;Y was detectable as early as 2 min post assay start. Its concentration increased until time point 45 min before slightly and slowly decreasing again. Shortened alkyne FAs were not detectable throughout the experiment, but their respective alkyne acyl-CARs became barely visible at later time points (30–90 min). At the TLC's origin of application a fluorescent band that likely corresponded to the alkyne acyl-CoAs was detected early (2 min) and remained present throughout the experiment, albeit fading in intensity after time point 45 min. Also some other alkyne metabolites were detectable during the experimental time window but could not be identified due to the lack of suitable TLC lipid standards.

Also the oxaalkyne tracer FA 17:0;Y;oxa was the only detectable lipid at the initial time point 0 min (Fig. 1D). A somewhat faster loss of FA 17:0;Y;oxa compared with FA 17:0;Y was observed during the early phase of the experiment (compare time point 15 min in Fig. 1D vs. 1C). For the oxaalkyne tracer, a timely staggered appearance of considerable amounts of labeled acyl-CARs with a clear hierarchical kinetics was observed (Fig. 1D). Whereas early time points showed CAR 17:0;Y;oxa as the main metabolite, a continuous shift toward shorter acyl-CARs became obvious for extended incubation times. During the experiment, the shortened FA 11:0;Y;oxa was accumulating, but only minor amounts of FA 9:0;Y or other labeled FAs could be observed. Putative oxaalkyne acyl-CoAs were detectable at the TLCs origin for all but the initial time
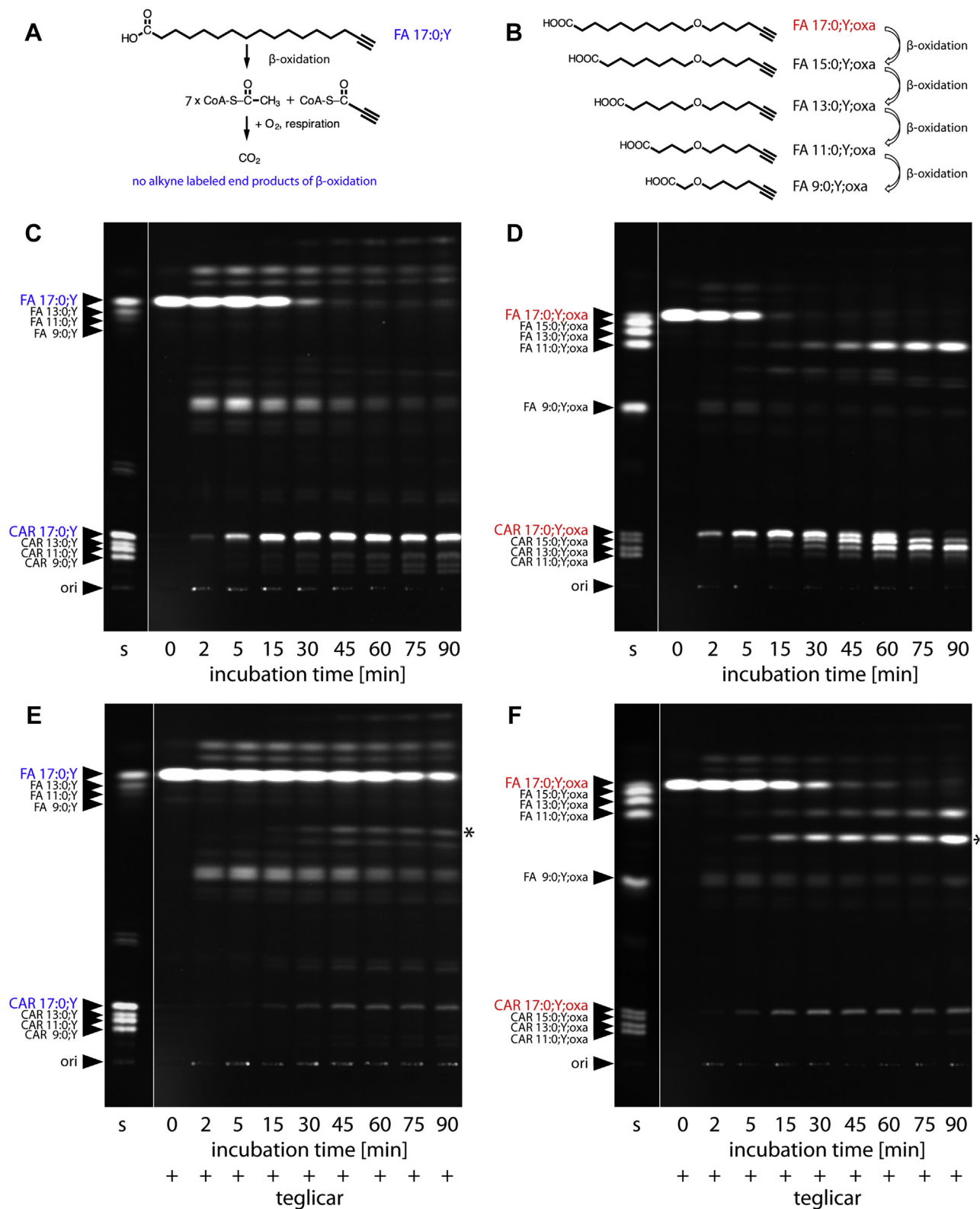
Fig. 1. Analysis of long-chain FA catabolism in liver lysate. A: After seven β-oxidation cycles the FA 17:0;Y yields seven molecules of acetyl-CoA and the instable propiolyl-CoA. B: After four β-oxidation cycles the FA 17:0;Y;oxa yields the end product FA 9:0;Y;oxa as CoA thioester containing a stable alkyne label. C–F, Liver lysate in assay buffer was preincubated at 33°C in absence (C, D) or presence (E, F) of 50 µM teglicar for 10 min. Assays were started by addition of 200 µM FA 17:0;Y (C, E) or FA 17:0;Y;oxa (D, F) and incubated for the indicated times. Lipids were click-reacted and analyzed by TLC. Fluorescent bands were identified by comigrating standards (s). An unidentified band (asterisk) accumulated upon teglicar treatment. ori, origin of application.

point. Also other metabolites could be observed but remained unidentified.

When these experiments were repeated in the presence of teglicar (33, 34), a reversible inhibitor of liver carnitine palmitoyltransferase 1 (CPT1), a different picture emerged (Fig. 1E and F). The input FAs yielded intense bands for extended time periods (compare time point 15 min in Fig. 1C–F) and their signals faded only slowly toward late time points (Fig. 1E and F). For both tracers and with the inhibitor present, the carnitine acylated by the respective full-length FA could clearly be observed albeit at a delayed time point and at a reduced concentration. However, no appreciable amounts of shortened acyl-CARs could be detected while an unidentified band, presumably the hydroxylated FA, accumulated (Fig. 1E and F, asterisk). In the presence of teglicar, the FA17:0;Y;oxa tracer still was metabolized to FA11:0;Y;oxa but not to the same extent (compare Fig. 1F vs. 1D). The putative acyl-CoAs of the alkyne and oxaalkyne FAs were detectable at the origin of the TLC and appeared not influenced by the presence of the inhibitor (compare Fig. 1C–E).

A quantitative analysis of the TLC data from the FA17:0;Y;oxa tracer in the absence or presence of teglicar was performed (Fig. 2). It illustrated the effect of the inhibitor on the relative amounts of input FA and FA11:0;Y;oxa (Fig. 2A), on the relative pool sizes of the labeled carnitin intermediates (Fig. 2B), as well as on the overall progression of β-oxidation (Fig. 2C). It also provided a measure of the inhibitor activity.

When the assay employing FA 17:0;Y;oxa was repeated without external supply of either CoA or carnitine, differences in the performance of β-oxidation were observed (supplemental Fig. S1). In the absence of CoA, the assay proceeded smoothly, but at lower speed, while omission of carnitine resulted in a strong accumulation of an unidentified band running at the expected position of hydroxylated FA 17:0;O;Y;oxa.

To extend the depth of the analysis, MS experiments were carried out. For optimal complement, the performed TLC and MS analyses used the same samples but internal standards were added for the latter. Since alkyne and oxaalkyne FAs and their metabolites possess unique masses, their MS signals can be readily distinguished from natural lipids. Our MS analysis focused on labeled FAs and acyl-CARs and included the products of each step of the β-oxidation cycle (i.e., the
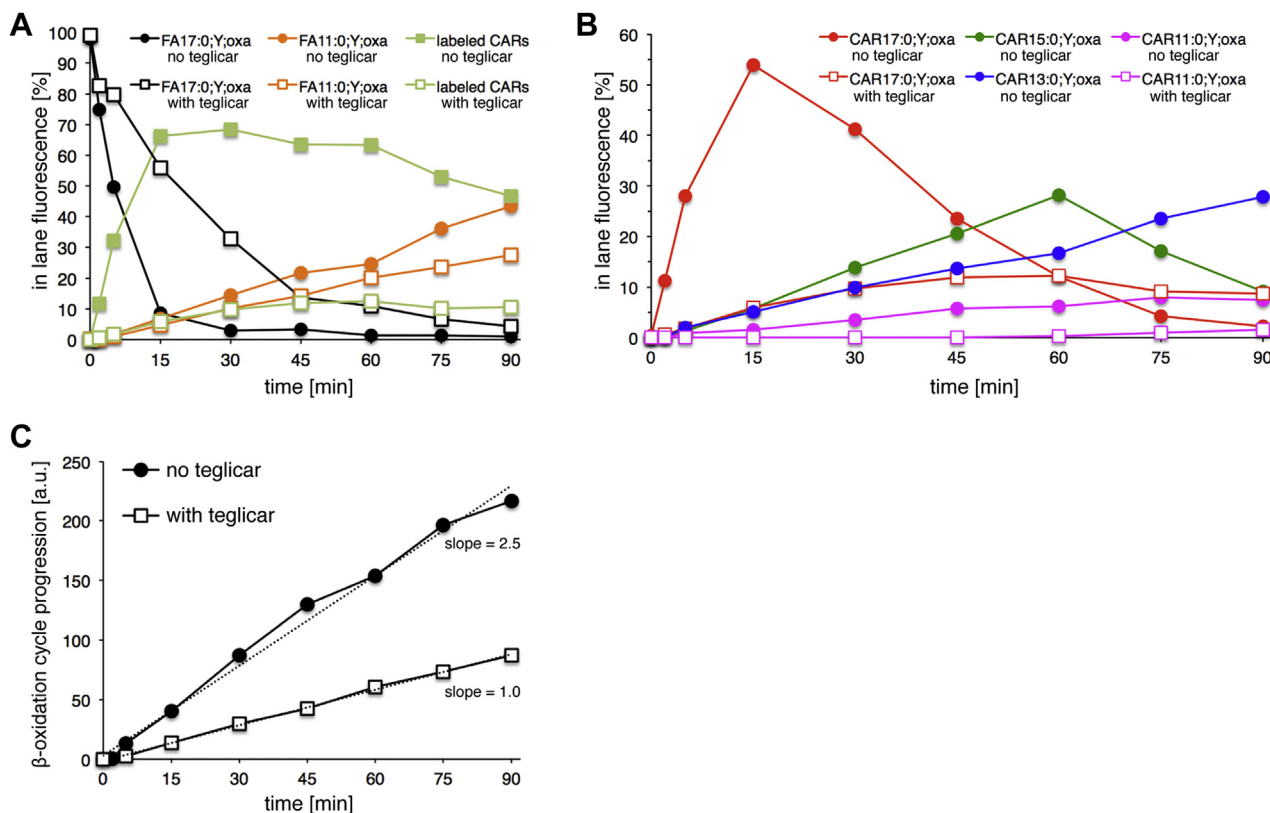
Fig. 2. Quantification of β-oxidation in liver lysate in the absence or presence of teglicar. Individual bands of the fluorescence images of the TLC plates in Fig. 1D and F were quantified by densitometry. A, B: The percentage of the total in lane fluorescence for each band was calculated and is plotted over time. Identified FAs and the sum of all labeled CARs (A) as well as the individual CAR species (B) are depicted. Note, that in the presence of the inhibitor no CAR15:0;Y;oxa or CAR13:0;Y;oxa could be detected. C: Progression analysis of β-oxidation. For each time point the advancement of oxidation was calculated by summing up the percentage of each cycles' products as defined by chain length (17, 15, 13, and 11 carbons) and multiplied by the respective cycle count (0, 1, 2, and 3, respectively). These values were normalized to time point zero and are plotted over time. Data indicate that β-oxidation proceeded with a nearly constant rate, which was reduced about 2.5-fold upon teglicar treatment.

various enoyl-, hydroxyacyl-, ketoacyl-, and the short-ened acyl-forms). For these, our analysis covered a molecule size range that included likely shortened metabolites as well as potential elongated products.

The MS data of samples incubated with the alkyne tracer FA 17:0;Y revealed that initially nearly 88% of the detected alkyne label was found in the FA pool and about 12% as acylated carnitines (Table 1 and supplemental Table S1). This distribution inverted to-ward the end of the experimental time window. The continuously fading FA 17:0;Y contributed most of the alkyne FA signal. In contrast, the increasing pool of labeled carnitines showed a wider diversity. Labeled acyl-, enoyl-, and hydroxyacyl-CARs accumulated throughout the time course. Although the chain length of 17 carbon atoms dominated the respective carnitine subclasses, also shortened chains were found accumu-lating. Interestingly, chains of 11 carbons were usually more abundant than that of 13 or 9 carbons within each subclass. Almost no signals for the elongated chain length of 19 or 21 carbons were found. A coincubation with teglicar for 30 min resulted in a strongly reduced catabolism of the input FA 17:0;Y.

The oxaalkyne tracer FA 17:0;Y;oxa displayed a fast turnover by β-oxidation (Table 2 and supplemental Table S2). While initially 96% of all detected labeled lipid was attributed to the input FA and 4% to the labeled acyl-CARs, the FA portion dropped to 24% within 15 min of incubation while that of the carnitines rose to 76%. At the latest time point, the signal for the input tracer was nearly lost and shortened chains especially FA 11:0;Y;oxa became the prevalent FAs. Only small amounts of FA 9:0;Y;oxa and almost no elongated FA 19:0;Y;oxa and FA 21:0;Y;oxa could be detected throughout the time series.

The MS analysis of the different oxaalkyne acyl-CARs confirmed the sequential appearance of the various species as observed by TLC with matching quantitative numbers (compare Table 2 vs. Figure 2). By MS, also enoylacyl-, hydroxyacyl-, and ketoacyl-CARs of different chain length were detected and the sequence of their appearance largely followed that of the respective acyl-CARs, but somewhat delayed. When β-oxidation was inhibited by teglicar, the turnover of the input FA 17:0;Y;oxa was markedly reduced and the hydroxylated metabolite FA 17:0;O;Y;oxa strongly accumulated. The latter finding substantiated the assumption that the accumulating band observed by TLC under these conditions (Fig, 1F, asterisk) indeed represents the hydroxylated FA.

Medium-chain FA β-oxidation in liver lysate

We next aimed to investigate the oxidative meta-bolism of medium-chain FAs by using an alkyne or oxaalkyne analogue of the saturated capric acid and TLC analysis (Fig. 3A–D). The assays were performed as above, but here FA 11:0;Y (Fig. 3A and C) or FA 11:0;Y;oxa (Fig. 3B and D) was used as input. The alkyne tracer FA 11:0;Y represented the only detectable band at time point 0 min and its signal faded quickly within 15 min of incubation (Fig. 3A). Minor amounts of elongation (FA 17:0;Y) and shortening products (FA 9:0;Y) became visible at early or late time points, respectively. Already after 2 min of incubation CAR 11:0;Y was observed, accumulated thereafter and yiel-ded the dominating band after 15–30 min. Shortened alkyne acyl-CARs appeared in a size- and time-dependent order. After 75 and 90 min incubation, the CAR 9:0;Y and putative CAR 7:0;Y were the prevalent acyl-CARs, while CAR 11:0;Y became much depleted. Minor amount of other labeled metabolites including putative acyl-CoAs could be detected. Coincubation with teglicar resulted in a reduced catabolism of the input FA 11:0;Y, illustrated by its delayed consumption and the diminished signals for labeled carnitines (Fig. 3C). With β-oxidation inhibited an unidentified lipid band, presumably hydroxylated FA 11:0;O;Y, star-ted to accumulate after 5 min of coincubation (Fig. 3C, asterisk). These TLC data were validated by a comple-mentary MS analysis (Table 3 and supplemental Table S3). It provided quantitative figures verifying the rapid loss of the input FA 11:0;Y within 15 min, the sequential appearance of various shortened labeled acyl-CARs and confirming the generation of CAR 7:0;Y at longer incubation times. It also verified the accu-mulation of the hydroxylated FA 11:0;O;Y upon coin-cubation with teglicar.

Compared with this tracer, a TLC analysis of the metabolic fate of the other analogue, FA 11:0;Y;oxa, yielded a quite different result. Both in the absence (Fig. 3B) and presence (Fig. 3D) of teglicar, the input FA signal was very stable over time with a minor signal of FA 9:0;Y;oxa becoming detectable after an incuba-tion time of 45 or 15 min, respectively. Even without inhibitor, only small amounts of labeled carnitines, mostly CAR 11:0;Y;oxa, could be seen throughout the time series (Fig. 3B). Coincubation with teglicar omitted a labeling of carnitines altogether (Fig. 3D). No other metabolites were clearly discernible. A comple-mentary MS analysis of samples incubated with FA 11:0;Y;oxa for 30 min in the absence or presence of teglicar was also performed (Table 4 and supplemental Table S4). The MS data confirmed the results from the TLC analysis and verified the presence of small amounts of FA 9:0;Y;oxa whose concentration increased upon teglicar coincubation. Conversely, the main metabolite CAR 11:0;Y;oxa was lost in the pres-ence of the inhibitor and no hydroxylated metabolite accumulated.

Unlike long-chain FAs whose transfer into mito-chondria necessitates prior formation of acyl-CoA and acyl-CAR, the medium-chain FAs may cross the mito-chondrial membranes in the nonesterified form. To assess the uptake mode, we separated mitochondria from the nonmitochondrial components by centrifu-gation. Using both fractions individually, assays

TABLE 1. Distribution of labeled lipid metabolites upon incubation of lysate with FA 17:0;Y. Here, the same assay samples as shown in Fig. 1 were analyzed by MS. Quantification was performed using internal standards. Data on all identified labeled lipid species are provided for the different incubation times. All time points of Fig. 1C and the 30 min time point of Fig. 1E are covered here. Numbers represent percentage of the labeled lipid species of the total label found within the lipid classes FA and CAR. These data also relate to supplemental Table S1

Identified Lipid	Time [min]									
	0	2	5	15	30	45	60	75	90	30 + teglicar
all FAs	**87.8**	**86.6**	**72.8**	**52.5**	**19.5**	**8.7**	**11.8**	**11.5**	**9.9**	**83.2**
saturated FAs	*78.1*	*82.4*	*66.3*	*45.4*	*13.3*	*3.7*	*4.1*	*3.2*	*3.3*	*81.9*
FA 21:0;Y	0.0	0.0	0.0	0.0	0.0	0.0	0.0	0.0	0.0	0.0
FA 19:0;Y	0.1	0.1	0.1	0.1	0.1	0.0	0.0	0.0	0.0	0.1
FA 17:0;Y	76.3	81.1	64.6	43.3	11.6	2.7	2.6	1.8	1.8	80.7
FA 15:0;Y	0.5	0.6	0.7	0.8	0.8	0.4	0.5	0.4	0.5	0.6
FA 13:0;Y	0.8	0.4	0.7	1.0	0.7	0.5	0.7	0.8	0.7	0.4
FA 11:0;Y	0.1	0.0	0.0	0.1	0.0	0.0	0.0	0.0	0.0	0.0
FA 9:0;Y	0.2	0.1	0.2	0.1	0.2	0.1	0.2	0.1	0.2	0.1
Enoyl-FAs	*0.4*	*0.2*	*0.3*	*0.3*	*0.5*	*0.3*	*0.5*	*0.5*	*0.4*	*1.2*
FA 21:1;Y	0.0	0.0	0.0	0.0	0.0	0.0	0.0	0.0	0.0	0.0
FA 19:1;Y	0.1	0.0	0.0	0.0	0.0	0.0	0.0	0.0	0.0	0.0
FA 17:1;Y	0.0	0.0	0.0	0.1	0.2	0.1	0.1	0.1	0.1	1.0
FA 15:1;Y	0.3	0.1	0.2	0.2	0.2	0.2	0.3	0.3	0.2	0.1
FA 13:1;Y	a	a	a	a	a	a	a	a	a	a
FA 11:1;Y	0.0	0.0	0.0	0.0	0.0	0.0	0.0	0.1	0.0	0.0
hydroxylated FAs	*7.4*	*3.1*	*4.8*	*5.2*	*4.5*	*3.6*	*5.7*	*6.1*	*4.9*	*3.5*
FA 21:0;O;Y	0.0	0.0	0.0	0.0	0.0	0.0	0.0	0.0	0.0	0.0
FA 19:0;O;Y	0.0	0.0	0.0	0.0	0.0	0.0	0.0	0.0	0.0	0.0
FA 17:0;O;Y	0.0	0.0	0.0	0.0	0.0	0.0	0.0	0.0	0.0	0.0
FA 15:0;O;Y	0.1	0.0	0.1	0.1	0.2	0.1	0.2	0.1	0.2	0.1
FA 13:0;O;Y	0.8	0.3	0.6	0.7	0.6	0.5	0.6	0.7	0.6	0.3
FA 11:0;O;Y	0.3	0.1	0.2	0.2	0.2	0.2	0.2	0.2	0.2	0.2
FA 9:0;O;Y	6.2	2.6	3.8	4.2	3.6	2.9	4.6	5.0	3.9	2.9
FA 7:0;O;Y	0.0	0.0	0.0	0.0	0.0	0.0	0.0	0.0	0.0	0.0
Keto-FAs[b]	*1.9*	*0.9*	*1.5*	*1.5*	*1.2*	*1.0*	*1.5*	*1.6*	*1.4*	*1.0*
FA 21:0;Y;oxo	0.0	0.0	0.0	0.0	0.0	0.0	0.0	0.0	0.0	0.0
FA 19:0;Y;oxo	0.0	0.0	0.0	0.0	0.0	0.0	0.0	0.0	0.0	0.0
FA 17:0;Y;oxo	0.3	0.2	0.3	0.2	0.3	0.2	0.3	0.3	0.3	0.2
FA 15:0;Y;oxo	0.2	0.1	0.2	0.2	0.2	0.1	0.2	0.3	0.2	0.1
FA 13:0;Y;oxo	0.8	0.4	0.7	0.7	0.5	0.4	0.7	0.8	0.6	0.4
FA 11:0;Y;oxo	0.0	0.0	0.0	0.0	0.0	0.0	0.0	0.0	0.0	0.0
FA 9:0;Y;oxo	0.4	0.2	0.3	0.3	0.3	0.2	0.3	0.3	0.3	0.2
all CARs	**12.2**	**13.4**	**27.2**	**47.5**	**80.5**	**91.3**	**88.2**	**88.5**	**90.1**	**16.8**
Acyl-CARs	*6.5*	*9.4*	*21.5*	*39.7*	*69.2*	*76.0*	*71.5*	*67.0*	*65.3*	*11.7*
CAR 21:0;Y	0.0	0.0	0.0	0.0	0.0	0.0	0.0	0.0	0.0	0.0
CAR 19:0;Y	0.0	0.0	0.0	0.0	0.0	0.0	0.1	0.1	0.1	0.0
CAR 17:0;Y	0.0	4.8	12.1	26.8	56.1	60.4	56.5	49.3	45.9	6.2
CAR 15:0;Y	0.0	0.9	2.9	5.8	7.9	8.5	6.8	7.9	8.0	0.1
CAR 13:0;Y	0.0	0.3	0.7	1.2	1.3	1.5	1.4	1.6	1.7	0.0
CAR 11:0;Y	6.4	3.1	5.2	4.9	2.7	3.8	5.0	6.0	6.2	5.2
CAR 9:0;Y	0.0	0.1	0.3	0.4	0.5	0.8	0.7	0.8	1.2	0.0
CAR 7:0;Y	0.0	0.1	0.3	0.6	0.6	1.0	1.0	1.3	2.1	0.0
Enoylacyl-CARs	*3.8*	*2.6*	*3.7*	*4.8*	*5.5*	*7.9*	*8.2*	*10.7*	*11.2*	*3.5*
CAR 21:1;Y	0.0	0.0	0.0	0.0	0.0	0.0	0.0	0.0	0.0	0.0
CAR 19:1;Y	0.1	0.0	0.0	0.0	0.0	0.0	0.0	0.0	0.1	0.0
CAR 17:1;Y	0.0	0.1	0.3	1.0	3.2	4.4	4.0	4.8	5.4	0.5
CAR 15:1;Y	0.0	0.0	0.1	0.2	0.5	0.9	1.0	1.7	1.8	0.0
CAR 13:1;Y	0.0	0.0	0.0	0.1	0.2	0.4	0.5	0.6	0.8	0.0
CAR 11:1;Y	3.7	2.5	3.2	3.3	1.5	2.2	2.5	3.4	3.1	3.0
CAR 9:1;Y	0.1	0.0	0.0	0.0	0.0	0.0	0.1	0.1	0.1	0.0
CAR 7:1;Y	0.0	0.0	0.0	0.0	0.0	0.0	0.0	0.0	0.1	0.0
Hydroxyacyl-CARs	*1.6*	*1.2*	*1.4*	*2.3*	*4.7*	*6.1*	*7.2*	*9.5*	*12.1*	*1.4*
CAR 21:0;O;Y	0.0	0.0	0.0	0.0	0.0	0.0	0.0	0.0	0.0	0.0
CAR 19:0;O;Y	0.0	0.0	0.0	0.0	0.0	0.0	0.0	0.0	0.0	0.0
CAR 17:0;O;Y	0.2	0.1	0.2	0.7	2.9	3.7	4.4	6.0	8.3	0.2
CAR 15:0;O;Y	0.1	0.0	0.1	0.3	1.0	1.4	1.4	1.7	1.9	0.1
CAR 13:0;O;Y	0.1	0.1	0.2	0.2	0.3	0.3	0.3	0.5	0.6	0.0
CAR 11:0;O;Y	1.2	0.8	0.8	1.0	0.5	0.7	1.0	1.1	1.1	1.1
CAR 9:0;O;Y	0.1	0.1	0.1	0.1	0.1	0.1	0.1	0.1	0.1	0.0
CAR 7:0;O;Y	0.0	0.1	0.1	0.1	0.1	0.0	0.1	0.1	0.1	0.0
Ketoacyl-CARs[b]	*0.3*	*0.3*	*0.5*	*0.8*	*1.1*	*1.3*	*1.3*	*1.3*	*1.5*	*0.2*
CAR 21:0;Y;oxo	0.0	0.0	0.0	0.0	0.0	0.0	0.0	0.0	0.0	0.0
CAR 19:0;Y;oxo	0.0	0.0	0.0	0.0	0.0	0.0	0.0	0.0	0.0	0.0
CAR 17:0;Y;oxo	0.0	0.0	0.0	0.0	0.0	0.0	0.0	0.0	0.0	0.0
CAR 15:0;Y;oxo	0.0	0.1	0.3	0.5	0.8	0.9	0.9	0.7	0.7	0.1

(continued)

TABLE 1. Continued

Identified Lipid	Time [min]									
	0	2	5	15	30	45	60	75	90	30 + teglicar
CAR 13:0;Y;oxo	0.0	0.1	0.1	0.1	0.1	0.2	0.2	0.3	0.4	0.0
CAR 11:0;Y;oxo	0.1	0.0	0.0	0.1	0.1	0.1	0.1	0.1	0.1	0.0
CAR 9:0;Y;oxo	0.1	0.1	0.1	0.1	0.1	0.1	0.1	0.1	0.1	0.0
CAR 7:0;Y;oxo	0.0	0.0	0.0	0.0	0.0	0.1	0.1	0.1	0.1	0.0

[a]*This species could not be analyzed due to an overlapping isomer peak of an unidentified compound.*
[b]*The ketoacyl form cannot be distinguished from the hydroxylated monounsaturated lipid by the MS routine used here.*

employing FA 11:0;Y were performed, but at the end of the incubation period, the mitochondria fraction was further subdivided by separating mitochondria from extra-mitochondrial volume. All samples were analyzed by TLC (**Fig. 4**A). The nonmitochondrial fraction (consisting of peroxisomes, microsomes, cytosol, and others) contained the bulk of the input FA, whose concentration strongly faded over the course of the experiment (Fig. 4A, left). This fraction also showed a strong and ever-increasing signal for CAR11:0;Y but hardly any signal for shortened acyl-CARs. At the lanes' origin putative acyl-CoAs with fluctuating signal intensities were observed. Mitochondria did not show appreciable amounts of acyl-CoAs but various acyl-CARs, including shortened ones. The amount of mitochondrial FA 11:0;Y was rather low compared with the nonmitochondrial fraction, but remained constant until after 40 min when the input tracer became strongly depleted. The extra-mitochondrial volume containing the secretion products of the mitochondria showed increasing signals for labeled acyl-CARs of different chain length, a band for putative acyl-CoAs, and the decreasing signal of the input FA 11:0;Y (Fig. 4A, right). A Western blot analysis on the mitochondrial and nonmitochondrial fractions used in the assays was performed and revealed that the signal for the mitochondrial acyl-CoA synthetase 1 (ACSM1), a mitochondrial matrix protein, was confined to the mitochondrial fraction (Fig. 4B). The detected bands fit the molecular weights of the long isoforms ACSM1-201 or -204 (65.3 kDa) and a short isoform, likely ACSM1-206 (28.1 kDa).

To collect more data on the interplay of medium-chain FA activation and β-oxidation, the assay was also performed under coincubation with triacsin C, an inhibitor of various acyl-CoA synthetases (35). In its presence, the pool of the input FA 11:0;Y in lysate remained fairly stable and no signal of putative acyl-CoAs at the origin of the TLC lane could be detected (supplemental Fig. S2A, left). The signals of the various labeled acyl-CARs were diminished compared to samples lacking triacsin C treatment, but their presence indicated ongoing β-oxidation of the medium-chain FA. In contrast, long-chain FA activation and catabolism were completely abolished by triacsin C (supplemental Fig. S2A, right).

An individual analysis of separated mitochondria and nonmitochondrial components employing FA 11:0;Y showed that triacsin C suppressed formation of labeled acyl-CoAs in the nonmitochondrial fraction and in the extra-mitochondrial volume (supplemental Fig. S2B, left and right). Mitochondria did not show labeled acyl-CoAs under both conditions (supplemental Fig. S2B, middle). In the presence of triacsin C, the mitochondria did not contain detectable amounts of CAR11:0;Y, but still produced (supplemental Fig. S2B, middle) and secreted (supplemental Fig. S2B, right) shortened acyl-CARs, albeit at a reduced rate.

Long- and medium-chain FA β-oxidation in primary hepatocytes

We next evaluated the applicability of alkyne and oxaalkyne FA tracing for investigations on β-oxidation in primary hepatocytes. Here, the fate of the FA tracer generally depends on overlaying anabolic and catabolic reactions, all embedded in the complex metabolism of a living cell. As cells closely interact with their environment, the cultivation media was included in the analysis.

First, primary hepatocytes were exposed to FA 17:0;Y for various incubation times in the absence or presence of teglicar and TLC analysis was performed (**Fig. 5**A). Already after 5 min labeled TG and after 20 min also labeled PC and two unidentified metabolites were observed. The intensity of these bands continuously increased while no labeled acyl-CARs or shortened FAs became detectable throughout the 6 h experimental time frame. Analysis of the cultivation media revealed a slowly depleting pool of input FA and the presence of labeled TG and PC at the latest time points. Coincubation with teglicar appeared to increase lipid biogenesis as the signals of labeled TG and PC in cells increased.

When hepatocytes were cultured in the presence of FA 17:0;Y;oxa only a single metabolite, labeled TG, could be detected in the cells throughout the experimental time frame (Fig. 5B). No labeled FA or CAR was observed. Coincubation with teglicar increased the cellular concentration of labeled TG throughout and gave rise to two other metabolites, labeled PC and an unidentified lipid, running at the expected height of doubly labeled TG. Analysis of the corresponding

TABLE 2. Distribution of labeled lipid metabolites upon incubation of lysate with FA 17:0;Y;oxa. Here, the same assay samples as shown in Fig. 1 were analyzed by MS. Quantification was performed using internal standards. Data on all identified labeled lipid species are provided for the different incubation times. All time points of Fig. 1D and the 30 min time point of Fig. 1F are covered here. Numbers represent percentage of the labeled lipid species of the total label found within the lipid classes FA and CAR. These data also relate to supplemental Table S2

Identified Lipid	Time [min]									
	0	2	5	15	30	45	60	75	90	30 + teglicar
all FAs	**96.2**	**59.0**	**53.1**	**23.6**	**20.8**	**19.4**	**20.0**	**22.7**	**32.2**	**81.8**
saturated FAs	*91.7*	*55.3*	*46.8*	*12.2*	*10.0*	*11.0*	*11.8*	*14.7*	*20.7*	*33.0*
FA 21:0;Y;oxa	0.0	0.0	0.0	0.0	0.0	0.0	0.0	0.0	0.0	0.0
FA 19:0;Y;oxa	0.1	0.1	0.1	0.1	0.1	0.1	0.1	0.1	1.0	0.1
FA 17:0;Y;oxa	89.2	53.3	43.2	6.9	2.7	1.8	1.1	0.3	0.3	26.7
FA 15:0;Y;oxa	0.2	0.2	0.6	1.1	1.3	1.7	1.7	1.3	0.9	0.3
FA 13:0;Y;oxa	0.8	0.7	1.2	1.5	1.8	1.9	2.2	3.0	3.6	1.3
FA 11:0;Y;oxa	0.7	0.5	1.0	2.1	3.5	4.6	5.9	8.8	13.1	3.2
FA 9:0;Y;oxa	0.8	0.6	0.7	0.6	0.7	0.9	0.8	1.3	1.9	1.3
Enoyl-FAs	*0.8*	*0.6*	*1.0*	*1.2*	*1.4*	*1.7*	*1.4*	*1.4*	*1.8*	*3.5*
FA 21:1;Y;oxa	0.0	0.0	0.0	0.0	0.0	0.0	0.0	0.0	0.0	0.0
FA 19:1;Y;oxa	0.0	0.0	0.0	0.0	0.0	0.1	0.1	0.0	0.3	0.0
FA 17:1;Y;oxa	0.3	0.3	0.6	0.8	1.0	1.1	0.8	0.6	0.5	2.6
FA 15:1;Y;oxa	0.1	0.1	0.1	0.1	0.1	0.2	0.2	0.2	0.3	0.1
FA 13:1;Y;oxa	0.3	0.2	0.2	0.2	0.2	0.2	0.2	0.4	0.6	0.5
FA 11:1;Y;oxa	0.1	0.0	0.1	0.0	0.1	0.1	0.1	0.2	0.1	0.2
hydroxylated FAs	*2.5*	*2.0*	*4.1*	*9.1*	*8.0*	*5.4*	*5.6*	*5.1*	*7.6*	*43.4*
FA 21:0;O;Y;oxa	0.0	0.0	0.0	0.0	0.0	0.0	0.0	0.0	0.0	0.0
FA 19:0;O;Y;oxa	0.0	0.0	0.0	0.0	0.0	0.0	0.0	0.0	0.2	0.0
FA 17:0;O;Y;oxa	0.0	0.2	2.2	7.2	5.4	2.7	2.4	0.5	0.3	40.9
FA 15:0;O;Y;oxa	0.0	0.0	0.0	0.0	0.0	0.0	0.0	0.0	0.0	0.0
FA 13:0;O;Y;oxa	0.3	0.2	0.2	0.3	0.7	1.1	1.3	2.1	3.5	0.4
FA 11:0;O;Y;oxa	0.3	0.2	0.2	0.2	0.3	0.3	0.3	0.3	0.4	0.3
FA 9:0;O;Y;oxa	1.9	1.4	1.3	1.3	1.7	1.4	1.5	2.1	3.2	1.7
Keto-FAs[a]	*1.2*	*1.1*	*1.2*	*1.1*	*1.3*	*1.3*	*1.3*	*1.5*	*2.0*	*2.0*
FA 21:0;Y;oxo;oxa	0.0	0.1	0.1	0.0	0.1	0.0	0.0	0.0	0.1	0.1
FA 19:0;Y;oxo;oxa	0.1	0.1	0.0	0.1	0.1	0.1	0.0	0.1	0.2	0.1
FA 17:1;Y;oxo;oxa	0.1	0.1	0.1	0.1	0.1	0.1	0.1	0.1	0.1	0.1
FA 15:0;Y;oxo;oxa	0.4	0.3	0.4	0.4	0.4	0.4	0.4	0.4	0.6	0.7
FA 13:0;Y;oxo;oxa	0.2	0.1	0.1	0.1	0.1	0.2	0.2	0.2	0.3	0.2
FA 11:0;Y;oxo;oxa	0.2	0.1	0.2	0.2	0.2	0.2	0.2	0.3	0.3	0.3
FA 9:0;Y;oxo;oxa	0.3	0.3	0.3	0.3	0.3	0.3	0.4	0.4	0.5	0.4
all CARs	**3.8**	**41.0**	**46.9**	**76.4**	**79.2**	**80.6**	**80.0**	**77.3**	**67.8**	**18.2**
Acyl-CARs	*0.3*	*33.4*	*41.3*	*66.0*	*61.8*	*58.3*	*57.2*	*49.0*	*40.2*	*11.5*
CAR 21:0;Y;oxa	0.0	0.0	0.0	0.0	0.0	0.0	0.0	0.0	0.0	0.0
CAR 19:0;Y;oxa	0.1	0.1	0.1	0.1	0.1	0.1	0.1	0.1	0.2	0.1
CAR 17:0;Y;oxa	0.1	30.9	36.1	53.1	38.4	21.1	15.2	0.8	0.1	11.1
CAR 15:0;Y;oxa	0.0	1.2	3.2	8.4	15.3	23.5	25.0	20.4	9.7	0.1
CAR 13:0;Y;oxa	0.0	1.0	1.7	4.1	7.7	13.2	16.3	26.2	27.4	0.0
CAR 11:0;Y;oxa	0.1	0.2	0.2	0.2	0.3	0.5	0.6	1.4	2.5	0.2
CAR 9:0;Y;oxa	0.0	0.0	0.0	0.0	0.0	0.1	0.1	0.1	0.2	0.0
Enoylacyl-CARs	*1.8*	*4.5*	*3.1*	*5.7*	*9.1*	*10.8*	*11.4*	*12.4*	*12.1*	*3.5*
CAR 21:1;Y;oxa	0.0	0.0	0.0	0.0	0.0	0.0	0.0	0.0	0.0	0.0
CAR 19:1;Y;oxa	0.0	0.0	0.0	0.0	0.0	0.0	0.0	0.0	0.0	0.0
CAR 17:1;Y;oxa	0.0	0.4	1.3	3.7	7.0	7.6	7.9	5.4	2.8	1.3
CAR 15:1;Y;oxa	0.0	0.0	0.0	0.1	0.5	1.1	1.2	2.9	3.7	0.0
CAR 13:1;Y;oxa	0.0	0.0	0.0	0.0	0.1	0.3	0.4	1.5	2.6	0.0
CAR 11:1;Y;oxa	1.8	4.0	1.8	1.7	1.5	1.8	1.9	2.7	2.9	2.2
CAR 9:1;Y;oxa	0.0	0.0	0.0	0.0	0.0	0.0	0.0	0.0	0.0	0.0
Hydroxyacyl-CARs	*0.9*	*1.6*	*1.4*	*3.3*	*6.3*	*8.7*	*8.4*	*11.6*	*10.5*	*2.4*
CAR 21:0;O;Y;oxa	0.0	0.0	0.0	0.0	0.0	0.0	0.0	0.0	0.0	0.0
CAR 19:0;O;Y;oxa	0.0	0.0	0.0	0.0	0.0	0.0	0.0	0.0	0.0	0.0
CAR 17:0;O;Y;oxa	0.0	0.3	0.5	1.9	3.9	4.2	5.0	7.1	6.3	0.4
CAR 15:0;O;Y;oxa	0.1	0.1	0.2	0.6	1.6	3.0	2.1	2.1	2.1	1.3
CAR 13:0;O;Y;oxa	0.1	0.1	0.1	0.2	0.4	0.8	0.8	1.2	0.9	0.1
CAR 11:0;O;Y;oxa	0.5	1.0	0.5	0.5	0.4	0.5	0.5	1.0	1.1	0.5
CAR 9:0;O;Y;oxa	0.1	0.1	0.0	0.0	0.0	0.0	0.0	0.1	0.1	0.0
Ketoacyl-CARs[a]	*0.8*	*1.5*	*1.1*	*1.5*	*2.0*	*2.8*	*3.0*	*4.4*	*5.1*	*0.8*
CAR 21:0;Y;oxo;oxa	0.0	0.0	0.0	0.0	0.0	0.0	0.0	0.0	0.0	0.0
CAR 19:0;Y;oxo;oxa	0.0	0.0	0.0	0.0	0.0	0.0	0.0	0.0	0.0	0.0
CAR 17:0;Y;oxo;oxa	0.1	0.2	0.3	0.6	1.2	1.5	1.3	0.9	1.3	0.2
CAR 13:0;Y;oxo;oxa	0.1	0.2	0.2	0.2	0.4	0.8	1.1	2.4	2.6	0.0
CAR 11:0;Y;oxo;oxa	0.4	0.9	0.5	0.5	0.3	0.4	0.4	0.8	0.9	0.6
CAR 9:0;Y;oxo;oxa	0.1	0.2	0.1	0.1	0.1	0.1	0.2	0.3	0.4	0.0

[a]*The ketoacyl form cannot be distinguished from the hydroxylated monounsaturated lipid by the MS routine used here.*
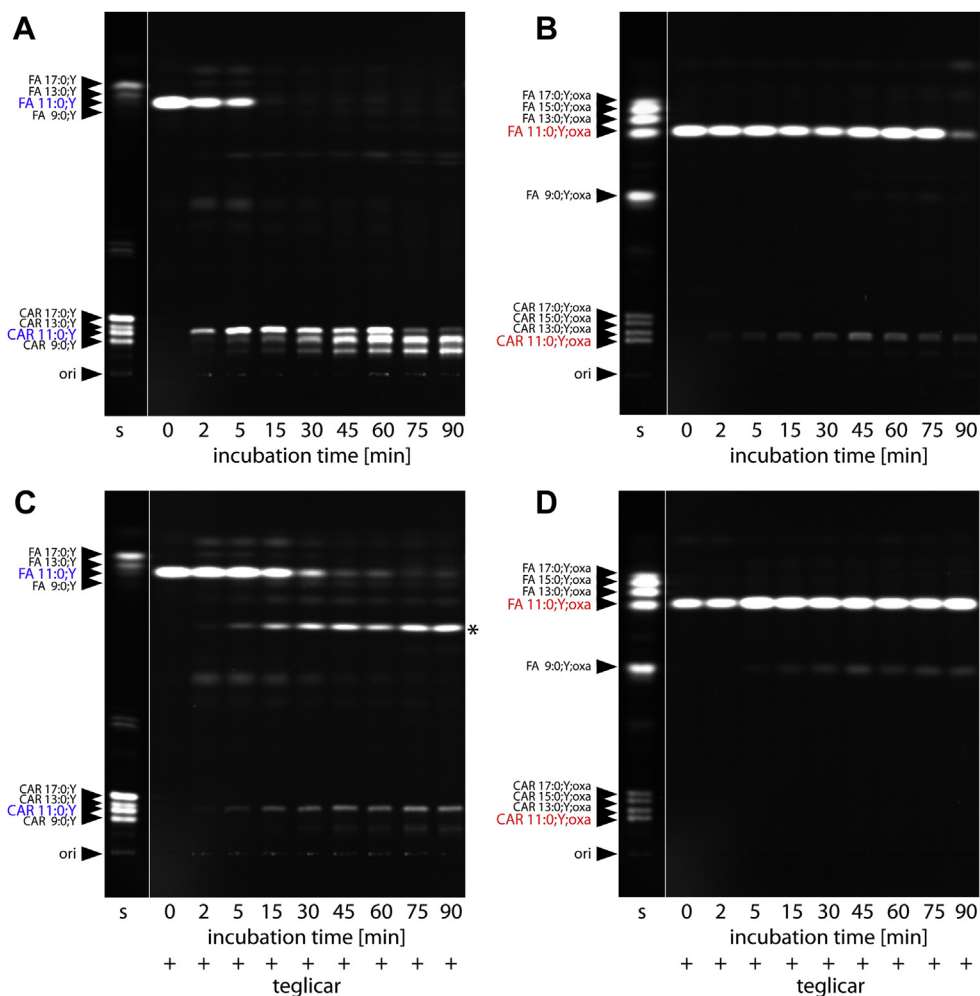
ASBMB

Fig. 3. Analysis of medium-chain FA catabolism in liver lysate. A–D, Liver lysate in assay buffer was preincubated at 33°C in absence (A, B) or presence (C, D) of 50 μM teglicar for 10 min. Assays were started by addition of 200 μM FA 11:0;Y (A, C) or FA 11:0;Y;oxa (B, D) and incubated for the indicated times. Lipids were click-reacted and analyzed by TLC. Fluorescent bands were identified by comigrating standards (s). An unidentified band (asterisk) accumulated upon coincubation of FA11:0;Y and teglicar. ori, origin of application.

culture media revealed the presence of the input FA as well as shortened oxaalkyne FAs with 11 or 9 carbon chains. In media FA 11:0;Y;oxa and FA 9:0;Y;oxa became detectable at time point 20 min or 1 h, respectively, and accumulated further. These β-oxidation products were generated by and secreted from hepatocytes as the incubation media alone lacked the necessary enzymatic activity and bands. After 6 h also labeled TG and PC, but no labeled acyl-CAR, were secreted from cells to the media. Teglicar did not profoundly influence the pool of secreted labeled lipids.

Next, the β-oxidation of medium-chain FA in living cells was investigated. Upon incubation of primary hepatocytes with either FA 11:0;Y (Fig. 5C) or FA 11:0;Y;oxa (Fig. 5D), a quite comparable picture emerged as the respective labeled TG was the only detectable metabolite in the cells. TG synthesis from FA 11:0;Y;oxa was slower than from FA 11:0;Y resulting in a delayed appearance of the respective TG band at time point 2 h rather than 20 min (compare Fig. 5C vs. 5D). Teglicar

increased the concentration of labeled TG in cells incubated with both tracers.

The media showed decreasing signals for both input FA tracers over time. Upon incubating cells for 6 h with FA 11:0;Y, the media contained acknowledgeable amounts of labeled TG (Fig. 5C), whereas only the FA 11:0;Y;oxa tracer yielded a shortened FA in the media (Fig. 5D). This FA 9:0;Y;oxa, a product of cellular β-oxidation appeared in the media already after 1 h and accumulated there over time. Both tracers produced additional bands that could not be identified due to the lack of suitable TLC standards. Teglicar had little to none influence on the pool of secreted labeled lipids.

A parallel MS analysis of the hepatocyte and media lipidomes upon cell incubation with alkyne (Table 5 and supplemental Table S5) or oxaalkyne FAs (Table 6 and supplemental Table S6) for 6 h in the absence or presence of teglicar was also performed. For all four FA tracers and in support of the TLC data, the MS quantification confirmed a relatively small pool of

TABLE 3.   Distribution of labeled lipid metabolites upon incubation of lysate with FA 11:0;Y. Here, the same assay samples as shown in Fig. 3 were analyzed by MS. Quantification was performed using internal standards. Data on all identified labeled lipid species are provided for the different incubation times. All time points of Fig. 3A and the 30 min time point of Fig. 3C are covered here. Numbers represent percentage of the labeled lipid species of the total label found within the lipid classes FA and CAR. These data also relate to supplemental Table S3

Identified Lipid	Time [min]									
	0	2	5	15	30	45	60	75	90	30 + teglicar
all FAs	**92.1**	**41.0**	**15.9**	**3.6**	**3.9**	**3.5**	**3.0**	**5.3**	**4.4**	**56.9**
saturated FAs	*83.5*	*35.5*	*11.3*	*0.9*	*0.7*	*0.6*	*0.7*	*0.9*	*0.6*	*21.1*
FA 21:0;Y	0.0	0.0	0.0	0.0	0.0	0.0	0.0	0.0	0.0	0.0
FA 19:0;Y	0.1	0.0	0.0	0.0	0.0	0.0	0.0	0.0	0.0	0.1
FA 17:0;Y	0.2	0.1	0.1	0.1	0.1	0.1	0.1	0.1	0.1	0.2
FA 15:0;Y	0.1	0.0	0.0	0.0	0.0	0.0	0.0	0.0	0.0	0.1
FA 13:0;Y	0.5	0.3	0.3	0.2	0.2	0.1	0.2	0.3	0.2	0.5
FA 11:0;Y	82.3	34.9	10.7	0.5	0.2	0.2	0.2	0.1	0.0	18.7
FA 9:0;Y	0.2	0.1	0.1	0.1	0.2	0.2	0.2	0.4	0.3	1.6
FA 7:0;Y	0.0	0.0	0.0	0.0	0.0	0.0	0.0	0.0	0.0	0.0
Enoyl-FAs	*0.5*	*0.3*	*0.2*	*0.1*	*0.2*	*0.2*	*0.1*	*0.2*	*0.1*	*0.9*
FA 21:1;Y	0.0	0.0	0.0	0.0	0.0	0.0	0.0	0.0	0.0	0.0
FA 19:1;Y	0.2	0.1	0.0	0.0	0.0	0.0	0.0	0.0	0.0	0.0
FA 17:1;Y	0.0	0.0	0.0	0.0	0.0	0.0	0.0	0.0	0.0	0.0
FA 15:1;Y	0.2	0.1	0.1	0.1	0.1	0.1	0.1	0.1	0.1	0.2
FA 13:1;Y	a	a	a	a	a	a	a	a	a	a
FA 11:1;Y	0.1	0.0	0.0	0.0	0.1	0.0	0.0	0.0	0.0	0.7
FA 9:1;Y	0.1	0.0	0.0	0.0	0.0	0.0	0.0	0.1	0.0	0.0
hydroxylated FAs	*6.3*	*4.1*	*3.5*	*2.0*	*2.3*	*2.1*	*1.7*	*3.3*	*2.8*	*33.5*
FA 21:0;O;Y	0.0	0.0	0.0	0.0	0.0	0.0	0.0	0.0	0.0	0.0
FA 19:0;O;Y	0.0	0.0	0.0	0.0	0.0	0.0	0.0	0.0	0.0	0.0
FA 17:0;O;Y	0.1	0.1	0.1	0.0	0.0	0.0	0.0	0.0	0.0	0.1
FA 15:0;O;Y	0.1	0.0	0.0	0.0	0.0	0.0	0.0	0.0	0.0	0.1
FA 13:0;O;Y	0.5	0.3	0.2	0.2	0.2	0.1	0.1	0.2	0.2	0.4
FA 11:0;O;Y	0.2	0.3	0.6	0.5	0.3	0.2	0.2	0.2	0.1	28.2
FA 9:0;O;Y	3.8	2.6	1.7	0.9	1.3	1.1	1.0	2.0	1.7	3.1
FA 7:0;O;Y	1.6	0.8	0.7	0.4	0.5	0.6	0.3	0.7	0.8	1.6
Keto-FAs[b]	*1.8*	*1.1*	*0.8*	*0.6*	*0.7*	*0.6*	*0.5*	*0.9*	*0.7*	*1.4*
FA 21:0;Y;oxo	0.0	0.0	0.0	0.0	0.0	0.0	0.0	0.0	0.0	0.0
FA 19:0;Y;oxo	0.0	0.0	0.0	0.0	0.0	0.0	0.0	0.0	0.0	0.0
FA 17:0;Y;oxo	0.2	0.1	0.1	0.0	0.0	0.1	0.1	0.1	0.1	0.1
FA 15:0;Y;oxo	0.2	0.1	0.1	0.1	0.1	0.1	0.0	0.1	0.1	0.1
FA 13:0;Y;oxo	0.8	0.5	0.4	0.3	0.3	0.2	0.2	0.4	0.3	0.6
FA 11:0;Y;oxo	0.0	0.0	0.0	0.0	0.0	0.0	0.0	0.0	0.0	0.0
FA 9:0;Y;oxo	0.4	0.2	0.1	0.1	0.1	0.1	0.1	0.1	0.1	0.2
FA 7:0;Y;oxo	0.3	0.2	0.2	0.1	0.1	0.1	0.1	0.2	0.2	0.3
all CARs	**7.9**	**59.0**	**84.1**	**96.4**	**96.1**	**96.5**	**97.0**	**94.7**	**95.6**	**43.1**
Acyl-CARs	*3.6*	*55.3*	*79.3*	*87.3*	*82.2*	*80.6*	*82.8*	*74.4*	*75.7*	*37.7*
CAR 21:0;Y	0.0	0.0	0.0	0.0	0.0	0.0	0.0	0.0	0.0	0.0
CAR 19:0;Y	0.0	0.0	0.0	0.0	0.0	0.0	0.0	0.0	0.0	0.0
CAR 17:0;Y	0.0	0.0	0.0	0.0	0.0	0.0	0.0	0.0	0.0	0.0
CAR 13:0;Y	0.0	0.0	0.0	0.0	0.0	0.0	0.0	0.0	0.0	0.0
CAR 11:0;Y	3.5	47.7	66.8	59.9	39.1	25.1	31.0	7.3	3.8	32.9
CAR 9:0;Y	0.1	6.1	10.1	22.2	35.6	43.4	41.0	47.9	44.8	1.3
CAR 7:0;Y	0.0	1.6	2.4	5.2	7.5	12.1	10.8	19.1	27.0	3.5
Enoylacyl-CARs	*2.2*	*2.0*	*3.2*	*6.4*	*8.3*	*8.8*	*8.8*	*10.0*	*10.3*	*4.3*
CAR 19:1;Y	0.0	0.0	0.0	0.0	0.0	0.0	0.0	0.0	0.0	0.0
CAR 17:1;Y	0.0	0.1	0.1	0.1	0.1	0.0	0.1	0.0	0.0	0.1
CAR 15:1;Y	0.0	0.0	0.0	0.0	0.0	0.0	0.0	0.1	0.0	0.0
CAR 13:1;Y	0.0	0.0	0.0	0.0	0.0	0.0	0.0	0.0	0.1	0.0
CAR 11:1;Y	2.1	1.9	2.9	6.0	7.8	7.9	8.0	7.8	7.0	4.1
CAR 9:1;Y	0.0	0.0	0.0	0.1	0.3	0.7	0.5	1.9	2.9	0.0
CAR 7:1;Y	0.0	0.1	0.1	0.1	0.1	0.1	0.1	0.2	0.3	0.1
Hydroxyacyl-CARs	*1.7*	*1.4*	*1.3*	*2.1*	*4.1*	*5.4*	*3.9*	*7.9*	*7.5*	*0.9*
CAR 21:0;O;Y	0.0	0.0	0.0	0.0	0.0	0.0	0.0	0.0	0.0	0.0
CAR 19:0;O;Y	0.0	0.0	0.0	0.0	0.0	0.0	0.0	0.0	0.0	0.0
CAR 17:0;O;Y	0.4	0.1	0.3	0.2	0.9	0.8	0.5	1.0	0.6	0.1
CAR 15:0;O;Y	0.1	0.1	0.1	0.3	0.6	0.9	0.5	0.9	0.6	0.1
CAR 13:0;O;Y	0.2	0.2	0.2	0.2	0.6	0.9	0.5	1.3	1.2	0.0
CAR 11:0;O;Y	0.7	0.7	0.5	1.1	1.7	2.6	2.1	4.0	4.0	0.6
CAR 9:0;O;Y	0.2	0.2	0.1	0.1	0.2	0.2	0.1	0.6	0.9	0.0
CAR 7:0;O;Y	0.1	0.1	0.0	0.1	0.0	0.0	0.0	0.1	0.2	0.0
Ketoacyl-CARs[b]	*0.4*	*0.3*	*0.4*	*0.6*	*1.4*	*1.6*	*1.5*	*2.4*	*2.2*	*0.2*
CAR 19:0;Y;oxo	0.0	0.0	0.0	0.0	0.0	0.0	0.0	0.0	0.0	0.0
CAR 17:0;Y;oxo	0.2	0.1	0.2	0.3	0.8	0.8	0.5	1.0	0.6	0.1
CAR 13:0;Y;oxo	0.1	0.1	0.1	0.1	0.2	0.2	0.1	0.3	0.3	0.0

(continued)

TABLE 3. Continued

Identified Lipid	Time [min]									
	0	2	5	15	30	45	60	75	90	30 + teglicar
CAR 11:0;Y;oxo	0.0	0.0	0.0	0.2	0.3	0.4	0.6	0.6	0.5	0.0
CAR 9:0;Y;oxo	0.1	0.1	0.1	0.1	0.1	0.2	0.2	0.4	0.5	0.0
CAR 7:0;Y;oxo	0.0	0.0	0.0	0.0	0.0	0.0	0.0	0.1	0.2	0.0

[a]*This species could not be analyzed due to an overlapping isomer peak of an unidentified compound.*
[b]*The ketoacyl form cannot be distinguished from the hydroxylated monounsaturated lipid by the MS routine used here.*

labeled FAs (0.3%–2.3% of all detectable labeled lipids) and the nearly complete absence of labeled CARs in cells. Also, the majority of label was generally found in the cellular TG pool and the medium-chain FA tracers showed a more pronounced bias for TG over PC labeling than the long-chain tracers. The MS data displayed that both alkyne FAs yielded an about threefold higher relative labeling of the PC pool than their oxaalkyne siblings. Other lipid classes were labeled only to a small extent by all four tracers.

In the cultivation media, the presence of the input alkyne FA was accompanied by substantial amounts of labeled TG (Table 5 and supplemental Table S5). While the signal of the long-chain FA17:0;Y dominated (78% of all label) over that of labeled TG (17%) and no other labeled FAs were found, the input mid-chain FA11:0;Y only contributed 17% of the total label and elongated FAs and TG accounted for 45% and 32%, respectively. For neither alkyne FA tracer, appreciable amounts of shortened FAs could be found in the media.

When the oxaalkyne FA tracers were used instead, the differences observed by TLC were confirmed by the MS data (Table 6 and supplemental Table S6). These media contained substantial amounts of shortened FAs, contributing 38% or 40% of the total label in samples using FA17:0;Y;oxa or FA11:0;Y;oxa tracer, respectively. Labeled TG accounted for less than 12% for both oxaalkyne FA tracers. Coincubation with teglicar nearly doubled the TG contribution but only slightly increased that of the shortened FAs in media. Of note, labeled acyl-CARs could not be detected in the media and cells although the amounts of endogenous unlabeled acyl-CARs considerably increased in both samples upon teglicar treatment (supplemental Table S7).

DISCUSSION

The liver is a major β-oxidizing tissue, and to study this process, an established experimental setup is based on freshly prepared liver lysate and radiotracers. We copied this setup but used oxaalkyne or alkyne FAs, which we introduce as tools to investigate FA catabolism. The novel oxaalkyne tracers are designed for this purpose and overcome a potential obstacle of alkyne FAs, which would not form a stable end product after the maximal number of β-oxidation cycles. In oxaalkyne FAs, an oxygen replaces a carbon atom in the chain conferring an advantage for the analysis. Unlike the radioactive FAs both oxaalkyne and alkyne tracers deliver only nonvolatile catabolites carrying a label. The vast majority of that label is concentrated in the lipid portion of all cell material and thus can together be subjected to analysis. TLC and MS analysis revealed the labeled lipid catabolites from the FA and acyl-CAR pools.

Comparison of the identified metabolites derived from the long-chain FA tracers FA17:0;Y;oxa or FA17:0;Y demonstrated the power of the new oxaalkyne FA tool. It allowed for the capture of various intermediates of the cyclic β-oxidation pathway including several shortened and oxidized acyl-CARs as well as FAs. These intermediates appeared and peaked sequentially, and the course of events showed a high qualitative correspondence to previously modeled and experimental data (36). Intrinsically, the occurrence of a great variety of acyl-CARs that likely are produced by the intramitochondrial CPT2 or potentially by carnitine acetyltransferase (CrAT) (37) is interesting as it points to an intense exchange of β-oxidation intermediates between mitochondria and cytosol. It also attests that β-oxidation of a single FA molecule does not proceed completely successively but rather generates a pool of intermediates that is sufficiently long-lived to be accessible for CPT2. This relates to the known sequential handling of metabolites by the different β-oxidation activities and may reflect the various enzymes' preferences for different acyl chain length. Surprisingly, the repeated processing of the oxaalkyne chain was not arrested to yield the shortest conceivable length of 9 carbons, but one cycle before and hence delivered chains of 11 carbons. This possibly indicates a hindrance of an enzymatic activity by the oxygen atom at the ε-position. Nonetheless, some continued processing also occurred delivering minor amounts of C9 chains. As end product after three cycles of β-oxidation of the FA17:0;Y;oxa, the assay produced FA11:0;Y;oxa that could be readily detected by TLC and MS. Labeled acyl-CoAs were also produced, but were not analyzed further.

As liver lysate lacks a fully functional metabolism replenishing all necessary cosubstrates, the assay

TABLE 4. Distribution of labeled lipid metabolites upon incubation of lysate with FA 11:0;Y;oxa. Here, the same assay samples as shown in Fig. 3 were analyzed by MS. Quantification was performed using internal standards. Data on all identified labeled lipid species are provided for the 30 min time points of Fig. 3C and D. Numbers represent percentage of the labeled lipid species of the total label found within the lipid classes FA and CAR. These data also relate to supplemental Table S4

Identified Lipid	Time [min]	
	30	30 + teglicar
all FAs	**60.4**	**90.5**
saturated FAs	*52.5*	*80.6*
FA 21:0;Y;oxa	0.0	0.0
FA 19:0;Y;oxa	0.1	0.2
FA 17:0;Y;oxa	0.3	0.4
FA 15:0;Y;oxa	0.2	0.2
FA 13:0;Y;oxa	1.2	1.4
FA 11:0;Y;oxa	48.3	72.6
FA 9:0;Y;oxa	2.4	5.7
Enoyl-FAs	*2.0*	*2.7*
FA 21:1;Y;oxa	0.0	0.0
FA 19:1;Y;oxa	0.0	0.0
FA 17:1;Y;oxa	0.7	0.8
FA 15:1;Y;oxa	0.1	0.2
FA 13:1;Y;oxa	0.5	0.8
FA 11:1;Y;oxa	0.3	0.6
FA 9:1;Y;oxa	0.3	0.4
hydroxylated FAs	*3.8*	*4.3*
FA 21:0;O;Y;oxa	0.0	0.0
FA 19:0;O;Y;oxa	0.0	0.1
FA 17:0;O;Y;oxa	0.1	0.1
FA 15:0;O;Y;oxa	0.1	0.1
FA 13:0;O;Y;oxa	0.4	0.6
FA 11:0;O;Y;oxa	0.4	0.6
FA 9:0;O;Y;oxa	2.8	2.9
Keto-FAs[a]	*2.1*	*2.9*
FA 21:0;Y;oxo;oxa	0.0	0.2
FA 19:0;Y;oxo;oxa	0.1	0.1
FA 17:1;Y;oxo;oxa	0.1	0.2
FA 15:0;Y;oxo;oxa	0.7	0.9
FA 13:0;Y;oxo;oxa	0.3	0.4
FA 11:0;Y;oxo;oxa	0.3	0.4
FA 9:0;Y;oxo;oxa	0.6	0.7
all CARS	**39.6**	**9.5**
Acyl-CARs	*32.0*	*1.1*
CAR 21:0;Y;oxa	0.0	0.0
CAR 19:0;Y;oxa	0.2	0.3
CAR 17:0;Y;oxa	0.0	0.0
CAR 11:0;Y;oxa	31.0	0.7
CAR 9:0;Y;oxa	0.7	0.1
Enoylacyl-CARs	*4.9*	*4.7*
CAR 21:1;Y;oxa	0.0	0.0
CAR 19:1;Y;oxa	0.0	0.0
CAR 11:1;Y;oxa	4.9	4.7
Hydroxyacyl-CARs	*2.5*	*3.5*
CAR 21:0;O;Y;oxa	0.0	0.0
CAR 19:0;O;Y;oxa	0.0	0.0
CAR 17:0;O;Y;oxa	0.3	0.1
CAR 15:0;O;Y;oxa	0.7	2.3
CAR 11:0;O;Y;oxa	1.4	1.1
Ketoacyl-CARs[a]	*0.2*	*0.1*
CAR 15:0;Y;oxo;oxa	0.2	0.1

[a]*The ketoacyl form cannot be distinguished from the hydroxylated mono-unsaturated lipid by the MS routine used here.*

contained external sources of CoA and carnitine. While without CoA supply β-oxidation continued albeit at a lower rate, a missing carnitine input abolished the formation of labeled acyl-CARs. Lacking free carnitine, CPT1 was unable to produce acyl-CARs for mitochondrial uptake via carnitine-acylcarnitine-translocase (CACT) and the FA17:0;Y;oxa tracer was instead hydroxylated extra-mitochondrially.

Also in the presence of teglicar, an inhibitor of liver CPT1 but not of muscle CPT1 or CPT2 (33, 34), the generation and mitochondrial import of CAR17:0;Y;oxa were hindered. However, as a residual signal of CAR17:0;Y;oxa was detectable, incomplete inhibition of CPT1 or the presence of another similar activity has to be taken into account. Nonetheless, teglicar slowed FA consumption and strongly reduced the production of shortened labeled acyl-CARs. Instead and as observed in assays omitting external carnitine, the hydroxylated FA17:0;O;Y;oxa accumulated. Its origin, however, remains unclear. In general, peroxisomal β-oxidation normally processing very long-chain FAs in mammals and operating independent of a carnitine shuttle (6, 9) has to be considered as a possible salvage pathway when the mitochondrial apparatus is inhibited by teglicar or by a lack of carnitine. However, as peroxisomal β-oxidation might explain the production of FA11:0;O;Y;oxa, it does not clarify the accumulation of hydroxylated FA17:0;O;Y;oxa.

Also for the evaluation of medium-chain FA catabolism an oxaalkyne tracer, FA11:0;Y;oxa, was developed and tested along its alkyne sibling FA11:0;Y. In accordance with data from the long-chain FA17:0;Y;oxa and substantiating an adverse effect of the ε-oxygen on an enzymatic activity, the shortening of FA11:0;Y;oxa to yield a chain length of nine carbons was minute. Conversely, consumption of the input FA11:0;Y;oxa was slow and only low amounts of labeled carnitines with a C9 chain were produced. Inhibition of CPT1 by teglicar stabilized the pool of the input FA further and blocked the formation of labeled acyl-CARs. Interestingly, the presence of the drug resulted in a slightly increased formation of the shortened FA9:0;Y;oxa. This observation may support the notions of a possible peroxisomal β-oxidation of medium-chain FAs (4, 6, 38) or that of an uptake of medium-chain FAs to mitochondria independently of the carnitine shuttle (7, 39, 40). Both processes remain active in the presence of the CPT1 inhibitor and may not generate labeled acyl-CARs. The peroxisomally produced FA9:0;Y;oxa could likely leave the organelle in a carnitine-independent fashion (41) although also peroxisomal carnitine-octanoyl transferases have been described (42, 43). In the light of the slow turnover of the tracer, however, the capacity for processing the FA11:0;Y;oxa in peroxisomes as in mitochondria appears low.

As the alkyne FA11:0;Y tracer does not feature an ε-oxygen, it may be regarded more suitable to assess medium-chain FA catabolism. Indeed, it was well accepted and processed by the β-oxidation machinery and delivered several traceable metabolites. As a main outcome, our data from this tracer support a model, where medium-chain FAs can undergo activation inside and outside of mitochondria by different acyl-CoA
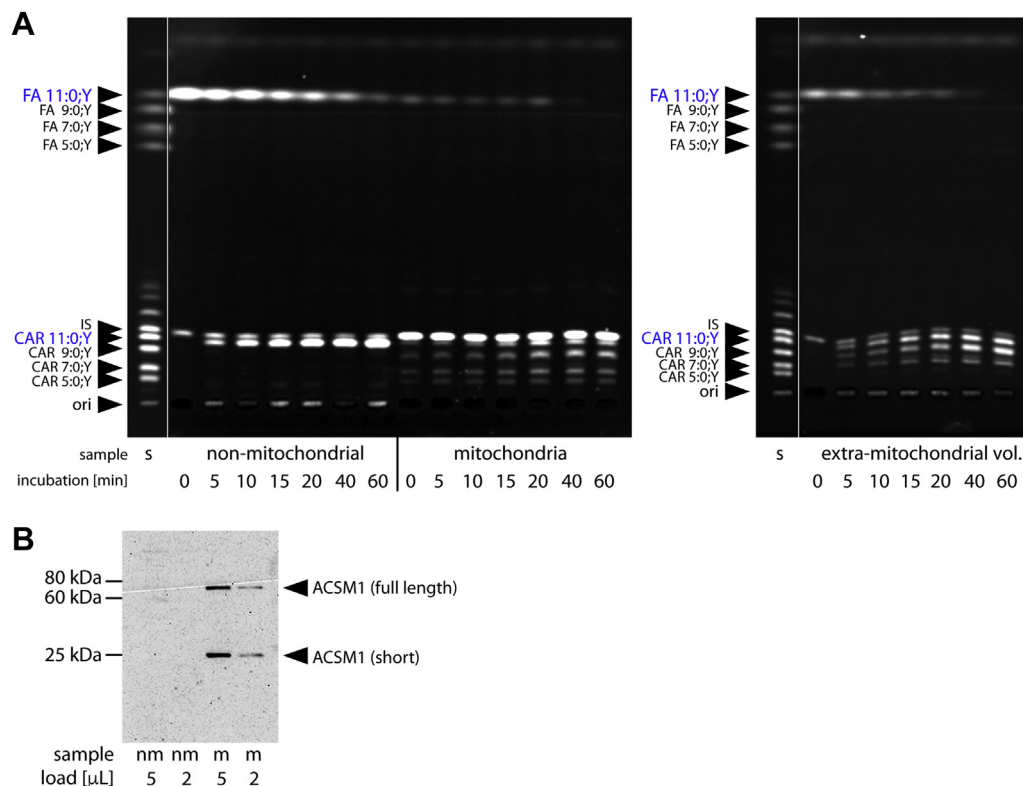
Fig. 4. Analysis of medium-chain FA catabolism in fractionated liver lysate. The liver lysate was divided in nonmitochondrial (nm) components and a mitochondria-enriched suspension (m) by centrifugation. A: Both fractions were separately preincubated at 37°C for 10 min. Assays were started by addition of 100 μM FA11:0;Y and incubated for the indicated times. Mitochondria from m-samples were pelleted and separated from supernatant (extra-mitochondrial volume). Lipids were click-reacted and analyzed by TLC. Fluorescent bands were identified by comigrating standards (s) and an internal standard (IS) served as reference as a sevenfold excess of the mitochondria samples were loaded to the TLC. ori, origin of application. B: The nm- and m-samples were analyzed by Western blotting probing for the distribution of the mitochondrial matrix protein ACSM1.

synthetases and can enter mitochondria in the form of free FAs or as carnitine esters. This idea is backed up by our finding that medium-chain FAs albeit at a reduced level still entered mitochondria when their activation was blocked by triacsin C. Also when the formation of acyl-CAR from acyl-CoA was inhibited by teglicar, medium-chain FAs had access to mitochondria but again to a lesser extent. The latter finding is also in line with earlier results using a different uptake inhibitor (4).

Judged by our data, at least in the liver, the majority of medium-chain FA activation occurs outside of mitochondria. This implies that cells have a larger cytosolic than mitochondrial pool of medium-chain acyl-CoA. In lysates, a great fraction of this acyl-CoA is converted to acyl-CAR for subsequent uptake into mitochondria. Likely, CPT1 located to the outer mitochondrial membrane is the main activity catalyzing this trans-esterification, albeit our fractionation experiments locate substantial amounts of CAR11:0;Y to the nonmitochondrial fraction. The latter may suggest the involvement of another acyl-CAR forming activity, potentially peroxisomal carnitine-octanoyl transferase (9, 42, 43), or contamination of this fraction with broken

mitochondria. The presence of intact and fully active mitochondria, however, appears unlikely as no shortened acyl-CARs were detectable and a Western blot analysis did not indicate the presence of the matrix protein ACSM1.

The nonmitochondrial fraction, although devoid of active mitochondria, largely used up the input FA within an hour of incubation. As no biosynthesis of neutral or phospholipids was observed, peroxisomal catabolism likely accounted for the observed medium-chain FA depletion. In line, triacsin C stabilized the nonmitochondrial FA pool by inhibiting acyl-CoA synthesis and therefore blocking peroxisomal β-oxidation. Peroxisomal β-oxidation is independent of carnitine-mediated transport but uses acyl-CoAs (6–9).

In parallel, triacsin C also hindered but did not block mitochondrial β-oxidation. Without the drug, the mitochondrial fraction contained only a small pool of FA11:0;Y and no detectable acyl-CoAs. However, triacsin C increased the former pointing to the existence of a short-lived pool of mitochondrial acyl-CoAs fueling β-oxidation. Despite this transiency, the shortened acyl-CoA gave rise to the production of the less transient
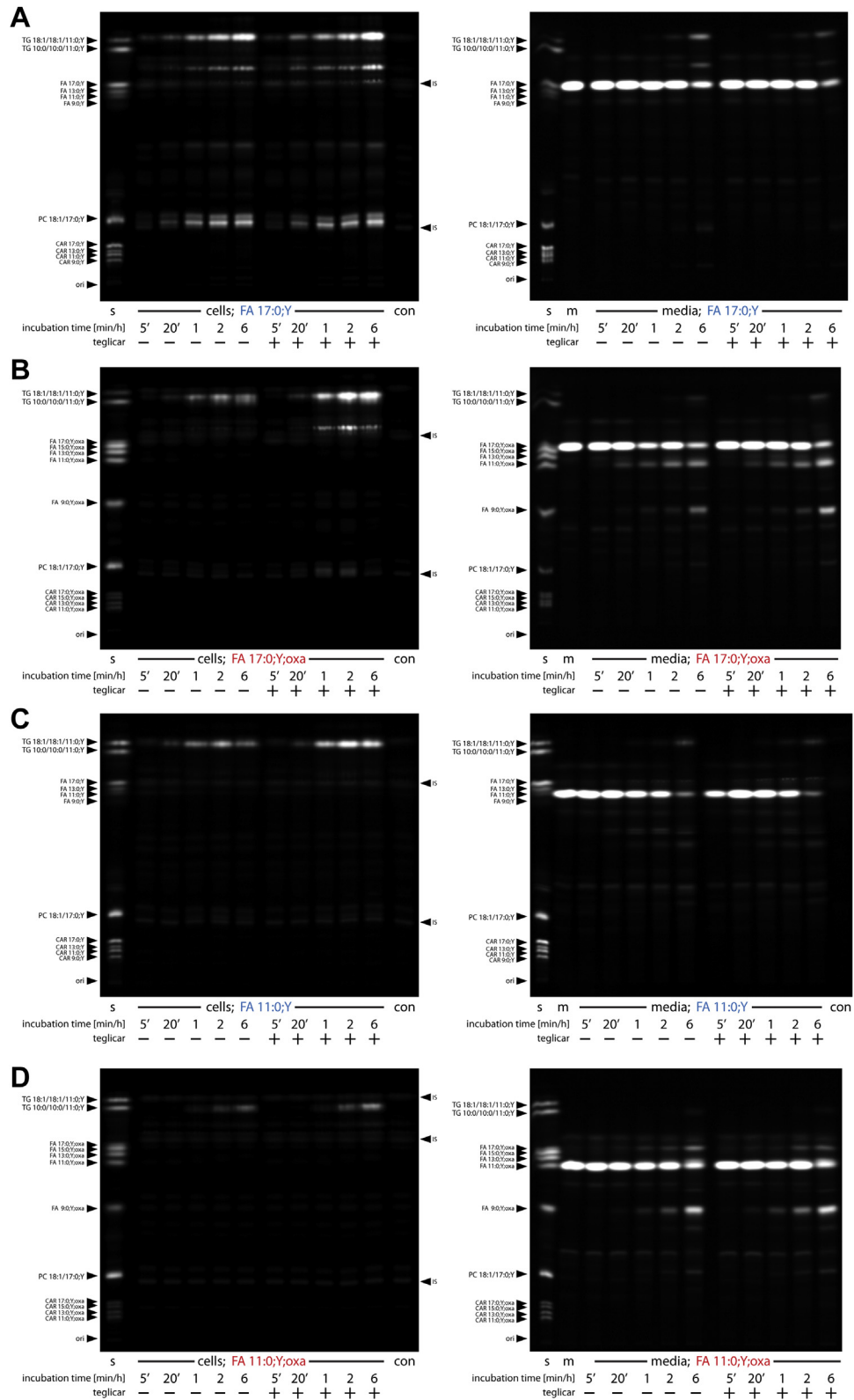
Fig. 5. Analysis of FA catabolism in living hepatocytes. Primary hepatocytes were preincubated in absence or presence of 50 μM teglicar for 10 min before addition of 50 μM FA 17:0;Y (A), FA 17:0;Y;oxa (B), FA 11:0;Y (C), or FA 11:0;Y;oxa (D) and incubation for the indicated times. Lipid extracts of cells (left panels) and media (right panels) were click-reacted and analyzed by TLC. Fluorescent bands were identified by comigrating TLC standards (s). Lipid extraction of cells was performed in the presence of internal standards (IS). Cells incubated in plain media (con) for 6 h and the incubation media containing the FA tracers (m) for 6 h were also analyzed. ori, origin of application.

TABLE 5. Distribution of labeled lipid metabolites in primary hepatocytes or cultivation media by MS. Cells were incubated with 50 µM FA 17:0;Y or FA 11:0;Y for 6 h in the absence or presence of teglicar. This data relates to Fig. 5A and C. Numbers represent percentage of the labeled lipid of the total label detected in 150,000 cells or 800 µl culture media as determined and quantified by MS. For the pools of labeled neutral and phospholipids, the sum of all detected species is shown. All individual species are quantified in supplemental Table S5

Identified Lipid	Cells				Media			
	17:0;Y	17:0;Y + teglicar	11:0;Y	11:0;Y + teglicar	17:0;Y	17:0;Y + teglicar	11:0;Y	11:0;Y + teglicar
all FAs	**2.3**	**1.9**	**1.6**	**1.1**	**80.0**	**86.0**	**64.9**	**53.9**
saturated FAs	*2.1*	*1.7*	*1.0*	*0.8*	*79.1*	*84.7*	*39.6*	*39.2*
FA 21:0;Y	0.0	0.1	0.1	0.1	0.0	0.0	2.4	0.0
FA 19:0;Y	0.3	0.4	0.2	0.1	1.1	2.0	4.3	1.4
FA 17:0;Y	1.7	1.2	0.7	0.5	77.8	82.5	14.6	6.2
FA 15:0;Y	0.0	0.0	0.0	0.0	0.3	0.2	0.3	0.2
FA 13:0;Y	0.0	0.0	0.0	0.0	0.0	0.0	1.1	0.9
FA 11:0;Y	0.0	0.0	0.1	0.0	0.0	0.0	17.0	30.5
FA 9:0;Y	0.0	0.0	0.0	0.0	0.0	0.0	0.0	0.0
FA 7:0;Y	0.0	0.0	0.0	0.0	0.0	0.0	0.0	0.0
Enoyl-FAs	*0.1*	*0.2*	*0.5*	*0.3*	*0.6*	*0.9*	*22.3*	*12.2*
FA 21:1;Y	0.0	0.0	0.1	0.0	0.0	0.0	2.3	0.4
FA 19:1;Y	0.1	0.1	0.4	0.2	0.3	0.5	19.5	10.6
FA 17:1;Y	0.0	0.1	0.0	0.0	0.3	0.4	0.0	0.0
FA 15:1;Y	0.0	0.0	0.0	0.0	0.0	0.0	0.0	0.0
FA 13:1;Y	0.0	0.0	0.0	0.0	0.0	0.0	0.0	0.0
FA 9:1;Y	0.0	0.0	0.0	0.0	0.0	0.0	0.4	1.0
hydroxylated FAs	*0.0*	*0.0*	*0.0*	*0.0*	*0.3*	*0.3*	*2.6*	*2.1*
FA 21:0;O;Y	0.0	0.0	0.0	0.0	0.0	0.0	0.0	0.0
FA 19:0;O;Y	0.0	0.0	0.0	0.0	0.1	0.2	0.0	0.0
FA 17:0;O;Y	0.0	0.0	0.0	0.0	0.1	0.2	0.5	0.3
FA 15:0;O;Y	0.0	0.0	0.0	0.0	0.0	0.0	0.0	0.0
FA 13:0;O;Y	0.0	0.0	0.0	0.0	0.0	0.0	0.2	0.2
FA 11:0;O;Y	0.0	0.0	0.0	0.0	0.0	0.0	1.9	1.6
FA 9:0;O;Y	0.0	0.0	0.0	0.0	0.0	0.0	0.0	0.0
FA 7:0;O;Y	0.0	0.0	0.1	0.1	0.0	0.0	0.0	0.0
Keto-FAs[a]	*0.0*	*0.0*	*0.0*	*0.0*	*0.0*	*0.0*	*0.4*	*0.5*
FA 21:0;Y;oxo	0.0	0.0	0.0	0.0	0.0	0.0	0.2	0.1
FA 19:0;Y;oxo	0.0	0.0	0.0	0.0	0.0	0.0	0.1	0.1
FA 17:0;Y;oxo	0.0	0.0	0.0	0.0	0.0	0.0	0.0	0.0
FA 11:0;Y;oxo	0.0	0.0	0.0	0.0	0.0	0.0	0.1	0.1
FA 9:0;Y;oxo	0.0	0.0	0.0	0.0	0.0	0.0	0.0	0.2
FA 7:0;Y;oxo	0.0	0.0	0.0	0.0	0.0	0.0	0.0	0.1
all CARs	**0.8**	**0.0**	**0.0**	**0.0**	**0.9**	**0.0**	**0.0**	**3.3**
Acyl-CARs	0.6	0.0	0.0	0.0	0.8	0.0	0.0	3.3
Car 17:0;Y	0.6	0.0	0.0	0.0	0.8	0.0	0.0	3.3
Enoylacyl-CARs	*0.2*	*0.0*	*0.0*	*0.0*	*0.1*	*0.0*	*0.0*	*0.0*
Car 17:1;Y	0.2	0.0	0.0	0.0	0.1	0.0	0.0	0.0
Hydroxyacyl-CARs	*0.1*	*0.0*	*0.0*	*0.0*	*0.1*	*0.0*	*0.0*	*0.0*
Car 17:0;O;Y	0.1	0.0	0.0	0.0	0.1	0.0	0.0	0.0
all CE x:y;Y	0.1	0.0	0.0	0.0	0.0	0.0	0.0	0.0
all TG x:y;Y	42.1	38.5	81.2	83.1	12.1	8.5	30.4	41.7
all TG x:y;2Y	12.8	16.4	0.9	1.0	4.6	3.4	1.3	0.7
all DG x:y;Y	1.8	3.0	0.8	0.8	0.2	0.1	0.9	0.6
all MG x:y;Y	0.0	0.0	0.0	0.0	0.0	0.0	0.1	0.0
all PE x:y;Y	4.5	5.1	0.9	0.5	0.1	0.1	0.0	0.0
all PE O-x:y;Y	0.0	0.0	0.0	0.0	0.0	0.0	0.1	0.2
all PC x:y;Y	26.8	23.6	13.6	12.5	2.3	1.3	1.8	2.5
all PC O-x:y;Y	0.0	0.0	0.0	0.0	0.0	0.0	0.2	0.1
all PA x:y;Y	0.3	0.3	0.0	0.0	0.0	0.0	0.0	0.0
all PI x:y;Y	3.9	4.5	0.5	0.4	0.2	0.1	0.0	0.1
all PS x:y;Y	5.3	6.5	0.5	0.6	0.5	0.4	0.0	0.0
all Cer x:y;Y	0.1	0.1	0.0	0.0	0.0	0.0	0.4	0.2

[a]*The keto-FAs cannot be distinguished from hydroxylated monounsaturated FAs by the MS routine used here.*

shortened acyl-CARs. They in turn did not accumulate strongly in the matrix but were secreted from the mitochondria. As pointed out by the FA 17:0;Y;oxa data and demonstrated in these fractionation experiments, mitochondria intensely exchange acyl-CARs with the cytosol. This result of ours links to CACT, an antiporter known to shuttle acyl-CARs to the cytosol especially if their intramitochondrial levels rise (1). In lysate, the

mitochondria are embedded in the virtually indefinite volume of the assay. Here, labeled lipids secreted from mitochondria escape further metabolic processing at other cellular organelles. Hence, the various secreted intermediates can easily be detected.

Contrasting this, the cytosol of intact cells represents a rather confined volume. Here the mitochondria-derived acyl-CARs can rapidly be trans-esterified to

TABLE 6. Distribution of labeled lipid metabolites in primary hepatocytes or cultivation media by MS. Cells were incubated with 50 μM FA 17:0;Y;oxa or FA 11:0;Y;oxa for 6 h in the absence or presence of teglicar. These data relate to Fig. 5B and D. Numbers represent percentage of the labeled lipid of the total label detected in 150,000 cells or 800 μl culture media as determined and quantified by MS. For the pools of labeled neutral and phospholipids, the sum of all detected species is shown. All individual species are quantified in supplemental Table S6

Identified Lipid	Cells				Media			
	17:0;Y;oxa	17:0;Y;oxa + teglicar	11:0;Y;oxa	11:0;Y;oxa + teglicar	17:0;Y;oxa	17:0;Y;oxa + teglicar	11:0;Y;oxa	11:0;Y;oxa + teglicar
all FAs	**0.4**	**0.8**	**0.4**	**0.3**	**86.5**	**77.3**	**96.5**	**93.9**
saturated FAs	*0.4*	*0.8*	*0.1*	*0.1*	*81.2*	*71.4*	*89.1*	*85.8*
FA 21:0;Y;oxa	0.0	0.0	0.0	0.0	0.1	0.0	0.0	0.0
FA 19:0;Y;oxa	0.1	0.1	0.0	0.0	6.0	1.7	0.0	0.0
FA 17:0;Y;oxa	0.2	0.6	0.0	0.0	42.1	19.2	0.0	0.1
FA 15:0;Y;oxa	0.0	0.1	0.0	0.0	0.1	0.2	0.0	0.0
FA 13:0;Y;oxa	0.0	0.0	0.0	0.0	0.3	0.6	0.2	0.2
FA 11:0;Y;oxa	0.0	0.0	0.1	0.1	24.4	23.7	49.4	39.6
FA 9:0;Y;oxa	0.0	0.0	0.0	0.0	8.1	26.0	39.5	45.9
Enoyl-FAs	*0.0*	*0.0*	*0.2*	*0.1*	*2.7*	*3.3*	*4.9*	*6.1*
FA 19:1;Y;oxa	0.0	0.0	0.0	0.0	0.0	0.0	0.0	0.0
FA 17:1;Y;oxa	0.0	0.0	0.0	0.0	0.1	0.0	0.0	0.0
FA 15:1;Y;oxa	0.0	0.0	0.0	0.0	0.0	0.0	0.0	0.0
FA 13:1;Y;oxa	0.0	0.0	0.0	0.0	0.1	0.0	0.1	0.1
FA 11:1;Y;oxa	0.0	0.0	0.2	0.1	2.5	3.2	4.8	5.9
FA 9:1;Y;oxa	0.0	0.0	0.0	0.0	0.0	0.0	0.1	0.1
hydroxylated FAs	*0.0*	*0.0*	*0.0*	*0.0*	*2.3*	*2.0*	*2.0*	*1.5*
FA 17:0;O;Y;oxa	0.0	0.0	0.0	0.0	0.3	0.1	0.0	0.0
FA 15:0;O;Y;oxa	0.0	0.0	0.0	0.0	0.1	0.0	0.0	0.0
FA 13:0;O;Y;oxa	0.0	0.0	0.0	0.0	0.7	0.4	0.6	0.5
FA 11:0;O;Y;oxa	0.0	0.0	0.0	0.0	1.3	1.4	1.3	1.0
FA 9:0;O;Y;oxa	0.0	0.0	0.0	0.0	0.0	0.0	0.0	0.0
Keto-FAs[a]	*0.0*	*0.0*	*0.1*	*0.1*	*0.3*	*0.6*	*0.5*	*0.5*
FA 21:0;Y;oxo;oxa	0.0	0.0	0.0	0.0	0.0	0.0	0.0	0.0
FA 15:0;Y;oxo;oxa	0.0	0.0	0.0	0.0	0.0	0.0	0.0	0.0
FA 13:0;Y;oxo;oxa	0.0	0.0	0.0	0.0	0.0	0.0	0.1	0.1
FA 11:0;Y;oxo;oxa	0.0	0.0	0.0	0.0	0.3	0.6	0.5	0.5
FA 9:0;Y;oxo;oxa	0.0	0.0	0.1	0.1	0.0	0.0	0.0	0.0
all CARs	**0.0**	**0.0**	**0.0**	**0.0**	**0.0**	**0.0**	**0.0**	**0.0**
all CE x:y;Y;oxa	0.0	0.0	0.0	0.0	0.0	0.0	0.0	0.0
all TG x:y;Y;oxa	87.8	70.9	94.9	92.7	11.1	21.1	5.2	9.8
all TG x:y;2Y;2oxa	2.6	14.1	0.0	0.0	0.4	4.8	0.0	0.1
all DG x:y;Y;oxa	0.9	1.1	0.6	0.5	0.1	0.3	0.2	0.5
all MG x:y;Y;oxa	0.0	0.0	0.0	0.0	0.0	0.0	0.0	0.0
all PE x:y;Y;oxa	0.0	0.1	0.0	0.0	0.0	0.1	0.0	0.1
all PE O-x:y;Y;oxa	0.0	0.0	0.0	0.0	0.0	0.0	0.0	0.0
all PC x:y;Y;oxa	7.5	11.0	4.1	6.4	1.0	2.0	0.2	0.6
all PC O-x:y;Y;oxa	0.0	0.1	0.0	0.0	0.0	0.0	0.1	0.2
all PA x:y;Y;oxa	0.1	0.1	0.0	0.0	0.0	0.0	0.0	0.0
all PI x:y;Y;oxa	0.0	0.1	0.0	0.0	0.0	0.0	0.0	0.0
all PS x:y;Y;oxa	0.6	1.6	0.0	0.0	0.0	0.0	0.0	0.0
all Cer x:y;Y;oxa	0.0	0.0	0.0	0.0	0.0	0.1	0.1	0.2

[a]*The keto-FAs cannot be distinguished from hydroxylated monounsaturated FAs by the MS routine used here.*

CoA yielding the respective acyl-CoAs, which participate in multiple metabolic pathways. Alternatively, a yet unidentified acyl-CAR exporter may secrete the acyl-CARs to the circulation (1). Hence, the fate of these metabolites depends on a complicate network of anabolic and catabolic reactions. Depending on the constantly changing circumstances in a cell, any single labeled molecule might be used for lipid biogenesis or can reenter β-oxidation. Even more complex, both processes occur simultaneously and at different cellular sites. This situation imposes a challenge for tracing experiments especially if following a sequence of reactions such as β-oxidation, which is a spatially and mechanistically complex pathway that constantly exchanges intermediates. It appears advantageous to sequester the label in a relatively narrow set of metabolites that is specific, fairly stable over time, and easy to follow. This is what the oxaalkyne tracers enable for. Hence, they proved advantageous over their alkyne siblings in our assays using living cells.

Indeed, in the cell-based assays employing the oxaalkyne FA, the hepatocytes took up the tracer, processed it by β-oxidation, and secreted the shortened FAs as products of catabolism to the culture media. Expectedly, some tracer was also subjected to anabolism, yielding primarily labeled TG, some of which was also secreted to the media presumably as lipoprotein particles.

Noteworthy, a coincubation with teglicar did not profoundly influence the pool of secreted labeled lipids but resulted in increased lipid biosynthesis especially of TG confirming earlier findings (25). These

results illustrate a metabolic rerouting of the tracers. With mitochondrial β-oxidation blocked, a stronger contribution of anabolic reactions as well as peroxisomal catabolic processing is indicated. The latter appears of sufficient capacity to maintain the secretion level of shortened FA. Of note, neither the cells nor the media accumulated hydroxylated FA metabolites in the presence of teglicar. This contrasts our findings in lysates where we discovered the accumulation of hydroxylated long- and medium-chain FAs when CPT1 activity was blocked. There, the hydroxylated FAs enriched either in the presence of teglicar or in the absence of carnitine, but not when FA activation was blocked by triacsin C. This finding is puzzling and may indicate that in intact cells, the FA blocked from mitochondrial entry is used in other pathways rather than in hydroxylation reactions. In lysates, it remains unclear whether the hydroxylated FAs under the different conditions are generated by the same enzyme and pathway. If postulated, an off-target inhibition of teglicar on the 3-hydroxyacyl-CoA dehydrogenase activities could account for the observed accumulation of hydroxylated FAs. However, as our experiments with lysates lacking the drug or omitting carnitine showed, also other enzymatic activities such as the cytochrome P450 protein family catalyzing FA hydroxylation have to be considered.

Apart from the interest in a detailed analysis of β-oxidation in basic research, there is also a clinical implication of the knowledge gained. Disturbance of β-oxidation results in severe clinical symptoms including liver dysfunction (44). The inability of the liver to oxidize FAs results in liver steatosis, impaired ketone production, and elevated secretion of acyl-CARs to the circulation. The latter is measured during newborn screening and in suspected patients to detect anomalies of mitochondrial FA metabolism (1, 45). Micromolar concentrations of several acyl-CARs are routinely found in blood of patients with genetic defects accumulating upstream metabolites. Release of acyl-CARs is usually viewed as a salvage mechanism to avoid trapping of CoA in blocked enzymatic pathways. In line, we also detected a strong increase in the secretion of natural acyl-CARs, mostly CAR 16:0 upon teglicar treatment, but not of labeled acyl-CARs, a difference possibly reflecting very unequal pool sizes of the natural versus tracer FA. It appears to be an attractive possibility that circulating acyl-CARs would have additional functions, in particular in signaling, because released acyl-CARs carry information about the metabolic status of major β-oxidizing tissues. In line with this concept, the brain-specific isoform CPT1c appears to be a metabolic regulator rather than a transporter component (46–48).

In summary, introducing novel oxaalkyne tracers and benefiting from alkyne click chemistry and highly sensitive detection procedures, this study for the first time evaluates β-oxidation with a comprehensive coverage of the involved FA and acyl-CAR intermediates. Using liver lysates and freshly isolated hepatocytes as well-established models, it delivered a detailed quantitative picture of long-chain and medium-chain FA catabolism to highlight metabolic differences.

Author ORCIDs

Lars Kuerschner https://orcid.org/0000-0003-4783-0442
Philipp Leyendecker https://orcid.org/0000-0002-4709-9218
Maria Fiedler https://orcid.org/0000-0002-2942-2915
Jennifer Saam https://orcid.org/0000-0002-7752-3761

REFERENCES

1. Houten, S. M., Violante, S., Ventura, F. V., and Wanders, R. J. (2016) The Biochemistry and Physiology of Mitochondrial Fatty Acid β-Oxidation and Its Genetic Disorders. *Annu. Rev. Physiol.* **78**, 23–44
2. Adeva-Andany, M. M., Carneiro-Freire, N., Seco-Filgueira, M., Fernandez-Fernandez, C., and Mourino-Bayolo, D. (2019) Mitochondrial β-oxidation of saturated fatty acids in humans. *Mitochondrion*. **46**, 73–90
3. Pégorier, J. P., Duée, P. H., Herbin, C., Laulan, P. Y., Bladé, C., Peret, J., and Girard, J. (1988) Fatty acid metabolism in hepatocytes isolated from rats adapted to high-fat diets containing long- or medium-chain triacylglycerols. *Biochem. J.* **249**, 801–806

4. Christensen, E., Hagve, T. A., Grønn, M., and Christophersen, B. O. (1989) Beta-oxidation of medium chain (C8-C14) fatty acids studied in isolated liver cells. *Biochim. Biophys. Acta.* **1004**, 187–195

5. Papamandjaris, A. A., MacDougall, D. E., and Jones, P. J. (1998) Medium chain fatty acid metabolism and energy expenditure: obesity treatment implications. *Life Sci.* **62**, 1203–1215

6. Hunt, M. C., Siponen, M. I., and Alexson, S. E. (2012) The emerging role of acyl-CoA thioesterases and acyltransferases in regulating peroxisomal lipid metabolism. *Biochim. Biophys. Acta.* **1822**, 1397–1410

7. Schönfeld, P., and Wojtczak, L. (2016) Short- and medium-chain fatty acids in energy metabolism: the cellular perspective. *J. Lipid Res.* **57**, 943–954

8. Van Veldhoven, P. P., and Mannaerts, G. P. (1999) Role and organization of peroxisomal beta-oxidation. *Adv. Exp. Med. Biol.* **466**, 261–272

9. Wanders, R. J., and Waterham, H. R. (2006) Biochemistry of mammalian peroxisomes revisited. *Annu. Rev. Biochem.* **75**, 295–332

10. Huynh, F. K., Green, M. F., Koves, T. R., and Hirschey, M. D. (2014) Measurement of fatty acid oxidation rates in animal tissues and cell lines. *Methods Enzymol.* **542**, 391–405

11. Thiele, C., Papan, C., Hoelper, D., Kusserow, K., Gaebler, A., Schoene, M., Piotrowitz, K., Lohmann, D., Spandl, J., Stevanovic, A., Shevchenko, A., and Kuerschner, L. (2012) Tracing fatty acid metabolism by click chemistry. *ACS Chem. Biol.* **7**, 2004–2011

12. Bertozzi, C. R. (2011) A decade of bioorthogonal chemistry. *Acc. Chem. Res.* **44**, 651–653

13. Kolb, H. C., Finn, M. G., and Sharpless, K. B. (2001) Click Chemistry: Diverse Chemical Function from a Few Good Reactions. *Angew. Chem. Int. Ed. Engl.* **40**, 2004–2021

14. Rostovtsev, V. V., Green, L. G., Fokin, V. V., and Sharpless, K. B. (2002) A stepwise huisgen cycloaddition process: copper(I)-catalyzed regioselective "ligation" of azides and terminal alkynes. *Angew. Chem. Int. Ed. Engl.* **41**, 2596–2599

15. Tornoe, C. W., Christensen, C., and Meldal, M. (2002) Peptidotriazoles on solid phase: [1,2,3]-triazoles by regiospecific copper(i)-catalyzed 1,3-dipolar cycloadditions of terminal alkynes to azides. *J. Org. Chem.* **67**, 3057–3064

16. Kuerschner, L., and Thiele, C. (2014) Multiple bonds for the lipid interest. *Biochim. Biophys. Acta.* **1841**, 1031–1037

17. Haberkant, P., and Holthuis, J. C. (2014) Fat & fabulous: bifunctional lipids in the spotlight. *Biochim. Biophys. Acta.* **1841**, 1022–1030

18. Laguerre, A., and Schultz, C. (2018) Novel lipid tools and probes for biological investigations. *Curr. Opin. Cell Biol.* **53**, 97–104

19. Bumpus, T. W., and Baskin, J. M. (2018) Greasing the Wheels of Lipid Biology with Chemical Tools. *Trends Biochem. Sci.* **43**, 970–983

20. Ancajas, C. F., Ricks, T. J., and Best, M. D. (2020) Metabolic labeling of glycerophospholipids via clickable analogs derivatized at the lipid headgroup. *Chem. Phys. Lipids.* **232**, 104971

21. Milne, S. B., Tallman, K. A., Serwa, R., Rouzer, C. A., Armstrong, M. D., Marnett, L. J., Lukehart, C. M., Porter, N. A., and Brown, H. A. (2010) Capture and release of alkyne-derivatized glycerophospholipids using cobalt chemistry. *Nat. Chem. Biol.* **6**, 205–207

22. Beavers, W. N., Serwa, R., Shimozu, Y., Tallman, K. A., Vaught, M., Dalvie, E. D., Marnett, L. J., and Porter, N. A. (2014) ω-Alkynyl lipid surrogates for polyunsaturated fatty acids: free radical and enzymatic oxidations. *J. Am. Chem. Soc.* **136**, 11529–11539

23. Robichaud, P. P., Poirier, S. J., Boudreau, L. H., Doiron, J. A., Barnett, D. A., Boilard, E., and Surette, M. E. (2016) On the cellular metabolism of the click chemistry probe 19-alkyne arachidonic acid. *J. Lipid Res.* **57**, 1821–1830

24. Thiele, C., Wunderling, K., and Leyendecker, P. (2019) Multiplexed and single cell tracing of lipid metabolism. *Nat. Methods.* **16**, 1123–1130

25. Wunderling, K., Leopold, C., Jamitzky, I., Yaghmour, M., Zink, F., Kratky, D., and Thiele, C. (2021) Hepatic synthesis of triacylglycerols containing medium-chain fatty acids is dominated by diacylglycerol acyltransferase 1 and efficiently inhibited by etomoxir. *Mol. Metab.* **45**, 101150

26. Jao, C. Y., Roth, M., Welti, R., and Salic, A. (2009) Metabolic labeling and direct imaging of choline phospholipids in vivo. *Proc. Natl. Acad. Sci. U. S. A.* **106**, 15332–15337

27. Yaghmour, M. H., Thiele, C., and Kuerschner, L. (2021) An advanced method for propargylcholine phospholipid detection by direct-infusion MS. *J. Lipid Res.* **62**, 100022

28. Matt, C., Wagner, A., and Mioskowski, C. (1997) Novel Transformation of Primary Nitroalkanes and Primary Alkyl Bromides to the Corresponding Carboxylic Acids. *J. Org. Chem.* **62**, 234–235

29. Christophersen, B. O., and Bremer, J. (1972) Carnitine esters of unsaturated fatty acids. Preparation and some aspects of their metabolism. *Biochim. Biophys. Acta.* **260**, 515–526

30. Berry, M. N., and Friend, D. S. (1969) High-yield preparation of isolated rat liver parenchymal cells: a biochemical and fine structural study. *J. Cell Biol.* **43**, 506–520

31. Herzog, R., Schwudke, D., Schuhmann, K., Sampaio, J. L., Bornstein, S. R., Schroeder, M., and Shevchenko, A. (2011) A novel informatics concept for high-throughput shotgun lipidomics based on the molecular fragmentation query language. *Genome Biol.* **12**, R8

32. Patel, S. S., and Walt, D. R. (1988) Acetyl coenzyme A synthetase catalyzed reactions of coenzyme A with alpha, beta-unsaturated carboxylic acids. *Anal. Biochem.* **170**, 355–360

33. Giannessi, F., Pessotto, P., Tassoni, E., Chiodi, P., Conti, R., De Angelis, F., Dell'Uomo, N., Catini, R., Deias, R., Tinti, M. O., Carminati, P., and Arduini, A. (2003) Discovery of a long-chain carbamoyl aminocarnitine derivative, a reversible carnitine palmitoyltransferase inhibitor with antiketotic and antidiabetic activity. *J. Med. Chem.* **46**, 303–309

34. Conti, R., Mannucci, E., Pessotto, P., Tassoni, E., Carminati, P., Giannessi, F., and Arduini, A. (2011) Selective reversible inhibition of liver carnitine palmitoyl-transferase 1 by teglicar reduces gluconeogenesis and improves glucose homeostasis. *Diabetes.* **60**, 644–651

35. Vessey, D. A., Kelley, M., and Warren, R. S. (2004) Characterization of triacsin C inhibition of short-, medium-, and long-chain fatty acid: CoA ligases of human liver. *J. Biochem. Mol. Toxicol.* **18**, 100–106

36. van Eunen, K., Simons, S. M., Gerding, A., Bleeker, A., den Besten, G., Touw, C. M., Houten, S. M., Groen, B. K., Krab, K., Reijngoud, D. J., and Bakker, B. M. (2013) Biochemical competition makes fatty-acid β-oxidation vulnerable to substrate overload. *PLoS Comput. Biol.* **9**, e1003186

37. Violante, S., Ijlst, L., Ruiter, J., Koster, J., van Lenthe, H., Duran, M., de Almeida, I. T., Wanders, R. J., Houten, S. M., and Ventura, F. V. (2013) Substrate specificity of human carnitine acetyltransferase: Implications for fatty acid and branched-chain amino acid metabolism. *Biochim. Biophys. Acta.* **1832**, 773–779

38. Kasumov, T., Adams, J. E., Bian, F., David, F., Thomas, K. R., Jobbins, K. A., Minkler, P. E., Hoppel, C. L., and Brunengraber, H. (2005) Probing peroxisomal beta-oxidation and the labelling of acetyl-CoA proxies with [1-(13C)]octanoate and [3-(13C)]octanoate in the perfused rat liver. *Biochem. J.* **389**, 397–401

39. Aas, M., and Bremer, J. (1968) Short-chain fatty acid activation in rat liver. A new assay procedure for the enzymes and studies on their intracellular localization. *Biochim. Biophys. Acta.* **164**, 157–166

40. Aas, M. (1971) Organ and subcellular distribution of fatty acid activating enzymes in the rat. *Biochim. Biophys. Acta.* **231**, 32–47

41. Rokka, A., Antonenkov, V. D., Soininen, R., Immonen, H. L., Pirilä, P. L., Bergmann, U., Sormunen, R. T., Weckström, M., Benz, R., and Hiltunen, J. K. (2009) Pxmp2 is a channel-forming protein in Mammalian peroxisomal membrane. *PLoS One.* **4**, e5090

42. Markwell, M. A., McGroarty, E. J., Bieber, L. L., and Tolbert, N. E. (1973) The subcellular distribution of carnitine acyltransferases in mammalian liver and kidney. A new peroxisomal enzyme. *J. Biol. Chem.* **248**, 3426–3432

43. Farrell, S. O., Fiol, C. J., Reddy, J. K., and Bieber, L. L. (1984) Properties of purified carnitine acyltransferases of mouse liver peroxisomes. *J. Biol. Chem.* **259**, 13089–13095

44. Merritt, J. L.n., MacLeod, E., Jurecka, A., and Hainline, B. (2020) Clinical manifestations and management of fatty acid oxidation disorders. *Rev. Endocr. Metab. Disord.* **21**, 479–493

45. Wanders, R. J., Ruiter, J. P., IJLst, L., Waterham, H. R., and Houten, S. M. (2010) The enzymology of mitochondrial fatty acid beta-oxidation and its application to follow-up analysis of positive neonatal screening results. *J. Inherit. Metab. Dis.* **33**, 479–494

46. Price, N., van der Leij, F., Jackson, V., Corstorphine, C., Thomson, R., Sorensen, A., and Zammit, V. (2002) A novel brain-expressed protein related to carnitine palmitoyltransferase I. *Genomics*. **80**, 433–442

47. Obici, S., Feng, Z., Arduini, A., Conti, R., and Rossetti, L. (2003) Inhibition of hypothalamic carnitine palmitoyltransferase-1 decreases food intake and glucose production. *Nat. Med.* **9**, 756–761

48. Wolfgang, M. J., Kurama, T., Dai, Y., Suwa, A., Asaumi, M., Matsumoto, S., Cha, S. H., Shimokawa, T., and Lane, M. D. (2006) The brain-specific carnitine palmitoyltransferase-1c regulates energy homeostasis. *Proc. Natl. Acad. Sci. U. S. A.* **103**, 7282–7287